JGR Atmospheres

RESEARCH ARTICLE
10.1029/2019JD030634

Large-Amplitude Quasi-10-Day Waves in the Middle Atmosphere During Final Warmings

Y. Yamazaki[1] and V. Matthias[2]

[1]GFZ German Research Centre for Geosciences, Potsdam, Germany, [2]Potsdam Institute for Climate Impact Research, Potsdam, Germany

Key Points:
- Large-amplitude quasi-10-day waves are observed in the middle atmosphere following final warmings of 2016, 2015, and 2005
- Amplification of the wave is attributed to barotropic/baroclinic instability
- Not only the occurrence of SSW but also the seasonal timing of SSW is important for the wave variability

Correspondence to:
Y. Yamazaki,
yamazaki@gfz-potsdam.de

Citation:
Yamazaki, Y., & Matthias, V. (2019). Large-amplitude quasi-10-day waves in the middle atmosphere during final warmings. *Journal of Geophysical Research: Atmospheres*, *124*, 9874–9892. https://doi.org/10.1029/2019JD030634

Received 13 MAR 2019
Accepted 21 AUG 2019
Accepted article online 30 AUG 2019
Published online 4 SEP 2019

Correction added on 4 November 2020, after first online publication: Projekt Deal funding statement has been added.

Abstract Geopotential height measurements from the Aura Microwave Limb Sounder between 9- and 97-km altitudes during 2004–2018 are used to examine long-period (3–20 days) wave activity during the Northern Hemisphere winter and spring, with the primary focus on the response of normal mode Rossby waves in the middle atmosphere to sudden stratospheric warmings (SSWs). Unusually large westward propagating waves with Zonal Wave Number 1 and period ~10 days are observed at 55° latitude at the stratopause height (~48 km) and above following final warmings of 2016, 2015, and 2005. In each case, large-amplitude waves are observed for the duration of two to three wave cycles. Characteristics of the waves are in conformity with the second antisymmetric Rossby normal mode of Zonal Wave Number 1, or the quasi-10-day wave. The growth rate of the waves is significantly greater than the classical normal mode in the upper stratosphere (approximately 30–50 km) where instability conditions are met, indicating the amplification or excitation of the waves in that region. The response of the quasi-10-day wave during midwinter SSWs, and also during the spring transition without an SSW, is not as obvious as the wave response during final warmings. The results suggest that not only the occurrence of SSW but also the seasonal timing of SSW is an important factor for the transient variability of the quasi-10-day wave in the middle atmosphere.

1. Introduction

Classical wave theory predicts a series of normal mode (or resonant) oscillations that the Earth's atmosphere can support (see, e.g., reviews by Forbes, 1995; Kasahara, 1976; Madden, 1979, 2007; Salby, 1984). At periods longer than a day, oscillations of the second kind, or Rossby normal modes, can exist in the presence of the Earth's rotation. Each mode has a specific period τ and zonal wave number s, and its longitudinal and latitudinal structures are given by a sinusoidal function and Hough function, respectively. Most widely known are the oscillations with periods near 2, 5, 10, and 16 days, which are known as the 2-, 5-, 10-, and 16-day waves, respectively. Figure 1 illustrates the latitudinal structures of these waves, as predicted by the classical wave theory. The 2-, 5-, 10-, and 16-day waves are all westward propagating, and they are also referred to as traveling planetary waves or Rossby waves. The zonal wave number is $s = 1$ for the 5-, 10-, and 16-day waves, while the zonal wave number of the 2-day wave is mainly $s = 3$ (and sometimes $s = 2$ and $s = 4$). The 5- and 16-day waves are symmetric modes, for which perturbations in the zonal wind and geopotential height are symmetric about the equator, while the 2-day wave ($s = 3$) and 10-day wave are antisymmetric modes, for which the perturbations change the sign at the equator (see Figure 1). The energy of these waves decays with height from the surface, but the amplitude of perturbations in winds and geopotential height actually grows in the vertical due to the density decrease.

The classical wave theory is based on the assumption of a simple dissipationless atmosphere, where the mean fields are horizontally stratified and zonal mean winds are 0. In the presence of the dissipation and nonuniform background, the spectra of Rossby waves are suppressed, broadened, and shifted from the classical behavior (Kasahara, 1980; Salby, 1980, 1981a). Nevertheless, normal-mode-like oscillations can be observed in a realistic atmosphere around the expected oscillation periods (i.e., 2, 5, 10, 16 days) and zonal wave numbers, as well as with horizontal structures similar to the classical normal modes, as numerically demonstrated by Salby (1981b). In this case, however, pure resonant frequencies no longer exist, and each mode has a range of frequencies (or periods). Because of that, the term "quasi" is often inserted before the name of Rossby waves (i.e., quasi-2-day wave, quasi-5-day wave, etc.). Previous studies have confirmed the presence of Rossby normal modes in the middle atmosphere (15–100 km). The quasi-2-day wave and quasi-5-day

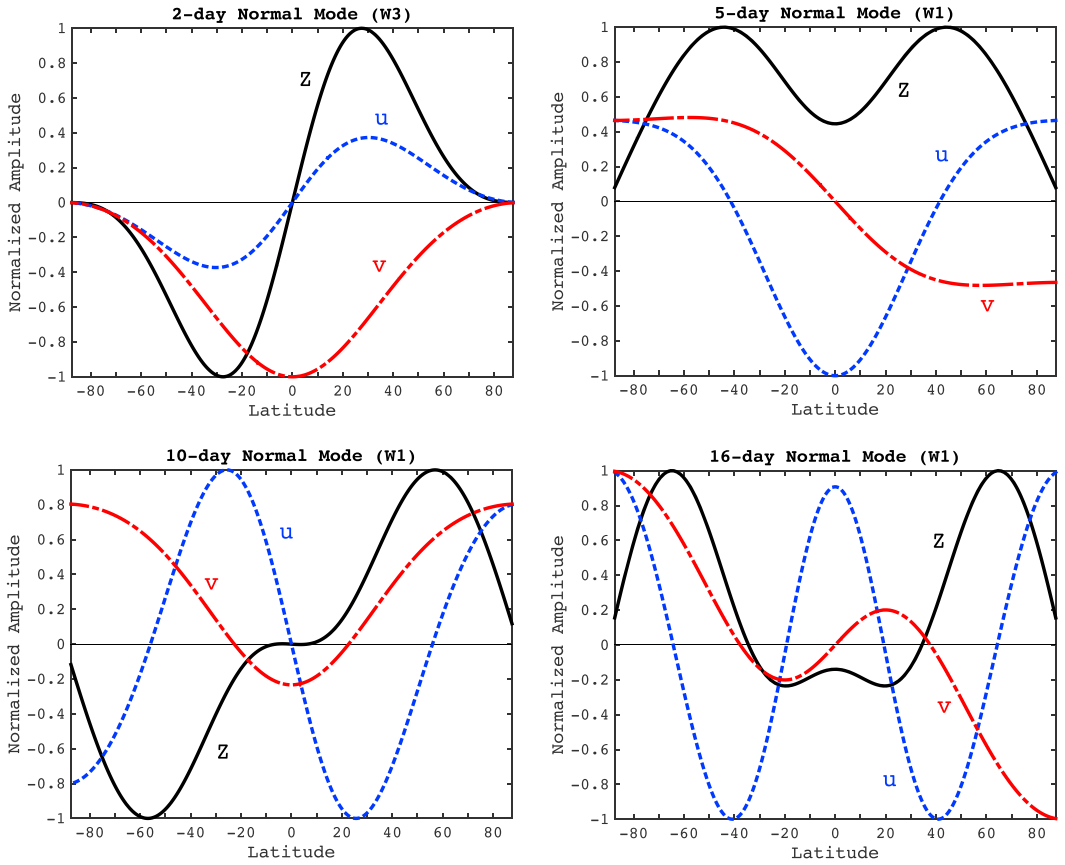

Figure 1. Latitudinal structures of geopotential height (Z, black), zonal wind velocity (u, blue), and meridional wind velocity (v, red) for the 2-day wave (3,0) mode, 5-day wave (1,1) mode, 10-day wave (1,2) mode, and 16-day wave (1,3) mode. The geopotential height amplitude is normalized by the maximum value of Z, while the velocity amplitudes are normalized by the largest value of u and v. Hough functions and velocity expansion functions are after Wang et al. (2016).

wave are particularly well studied using ground-based radar observations (e.g., Clark et al., 2002; Gu et al., 2013; Harris & Vincent, 1993; Jiang et al., 2008; Kishore et al., 2004; Kovalam et al., 1999; Muller & Nelson, 1978; Salby & Roper, 1980; Tsuda et al., 1988; Nozawa et al., 2003; Offermann et al., 2011; Pancheva et al., 2008; Sandford et al., 2008 and many others) and global satellite measurements (e.g., Burks & Leovy, 1986; Ern et al., 2013; Garcia et al., 2005; Gu et al., 2018, 2013; Forbes & Zhang, 2017; Hirota & Hirooka, 1984; Huang et al., 2013, 2017; John & Kumar, 2016; Lieberman et al., 2003; Limpasuvan & Wu, 2003, 2009; Limpasuvan et al., 2005; Rodgers, 1976; Rodgers & Prata, 1981; Merzlyakov et al., 2013; Moudden & Forbes, 2014; Pancheva et al., 2010, 2018a, 2018b; Riggin et al., 2006; Talaat et al., 2001; Tunbridge et al., 2011; Wu et al., 1993, 1994, 1996). The mean period of the quasi-2-day wave in the middle atmosphere is close to 2.0 days at low latitudes as shown, for example, by Gu et al. (2013) based on long-term mesospheric wind measurements at Hawaii. At middle and polar latitudes the period can be smaller or larger than 2 days, usually between 45 and 55 hr (e.g., McCormack et al., 2009; Nozawa et al., 2003). The period of the quasi-5-day wave in the middle atmosphere is often longer than 5 days, and the mean period is actually close to 6 days. For instance, Forbes and Zhang (2017) showed the mean period of the quasi-5-day wave to be 6.14 days (±0.26) based on the temperature measurements by the Sounding of the Atmosphere using Broadband Emission Radiometry (SABER) instrument on the Thermosphere-Ionosphere-Mesosphere Energetics and Dynamics (TIMED) satellite during 2002–2015. Accordingly, the quasi-5-day wave is also referred to as quasi-6-day wave. The quasi-16-day wave in the middle atmosphere has also been widely observed from the ground (e.g., Day & Mitchell, 2010; Espy et al., 1997; Forbes et al., 1995; Jiang et al., 2005; Kingsley et al., 1978; Luo et al., 2000, 2002; Mitchell et al., 1999; Williams & Avery, 1992) and from satellites (e.g., Day et al., 2011; John & Kumar, 2016; Hirooka & Hirota, 1985; Luo et al., 2002; McDonald et al., 2011). According to Forbes and Zhang (2017), the mean period of the quasi-16-day wave is 15.4 days (±0.26). The latitude and height

structures of the quasi-2-day, quasi-6-day, and quasi-16-day waves in the middle atmosphere have been successfully reproduced by numerical models (e.g., Chang et al., 2011; Forbes et al., 1995; Hagan et al., 1993; Gan et al., 2016; Koval et al., 2018; Liu et al., 2004; Meyer & Forbes, 1997; Miyoshi & Hirooka, 1999; Miyoshi, 1999; Palo et al., 1998, 1999; Pedatella et al., 2012; Yue et al., 2012).

The quasi-10-day wave is the least studied among the Rossby normal modes mentioned above. Nonetheless, the existence of the quasi-10-day wave in the middle atmosphere has been confirmed along with other waves. Hirooka and Hirota (1985) described characteristics of the quasi-10-day and quasi-16-day waves in geopotential height at 16- to 48-km altitude observed by the TIROS-N and NOAA-A satellites during 1979–1982. Both waves revealed a tendency to be larger in the winter hemisphere than in the summer hemisphere, with considerable irregular interannual variability. Jacobi et al. (1998) also noted the irregular nature of the interannual variations of these waves based on mesospheric wind measurements over central Europe. Hirooka (2000), using geopotential height measurements from the Upper Atmosphere Research Satellite, confirmed the presence of the quasi-10-day wave up to the mesopause altitude ~81 km during selected months in 1991 and 1992. Pancheva and Mukhtarov (2011) presented the seasonal and interannual variability of the quasi-16-day, quasi-10-day, and quasi-6-day waves at 20- to 120-km altitude during 2002–2007 using the TIMED/SABER temperature data. Forbes and Zhang (2015) examined the characteristics of the quasi-10-day wave in temperature observed by TIMED/SABER and found general consistency with the classical Rossby normal mode (1,2). According to their study, the mean period of the quasi-10-day wave in the middle atmosphere is 9.8 days (±0.4). John and Kumar (2016) also used TIMED/SABER temperature data to examine the quasi-16-day, quasi-10-day, and quasi-6-day waves. It was noted that the amplitudes of the westward and eastward propagating waves are comparable at period around $\tau = 10$ days.

Salby (1981a, 1981b) numerically examined Rossby normal modes under different atmospheric conditions. The results of his numerical experiments indicated that the upward propagation of Rossby waves depends strongly on the background atmosphere. It was shown that the distribution of the zonal mean flow is a particularly important factor for the Rossby wave propagation in the middle atmosphere. Salby's results hinted at the possibility that transient changes might occur in Rossby waves when the middle atmosphere is disturbed such as during sudden stratospheric warming (SSW) events. SSWs are large-scale disturbances in the middle atmosphere that take place at high latitudes, mostly in the Northern Hemisphere, during winter (e.g., Andrews et al., 1987; Labitzke & Van Loon, 1999). During an SSW event, the polar temperature in the stratosphere rapidly increases and the stratospheric polar jet weakens or even reverses direction. Liu et al. (2004), using a general circulation model, studied how temporal changes in the zonal mean zonal wind affect the propagation characteristics of the quasi-6-day wave, which in turn lead to amplification/suppression of the wave in the middle atmosphere. Although Liu et al. (2004) focused mainly on seasonal changes, they also predicted that the amplitude of the quasi-6-day wave in the middle atmosphere might enhance during SSW events in late winter, when the zonal mean flow in the stratosphere and mesosphere reverses and the middle atmosphere in the high-latitude region becomes unstable.

Possible influences of SSWs on Rossby normal modes have been addressed in many observational studies. Hirooka and Hirota (1985) noted that the quasi-10-day wave is enhanced in the stratosphere during late February to early March 1980, coinciding with the reversal of the stratospheric polar jet. Dowdy et al. (2004) and Espy et al. (2005) observed a large-amplitude west propagating wave with zonal wave number $s = 1$ and period τ ~14 days at 70- to 100-km altitude in the high latitudes of the Southern Hemisphere during the Antarctic SSW event of September 2002. Pancheva et al. (2008) examined long-period waves ($\tau = 5$–30 days) in the middle atmosphere during the winter of 2003–2004. They found enhanced wave activity around periods τ ~16 days and τ ~23 days during the SSW event of January 2004. Day et al. (2011) reported that the amplitude of the quasi-16-day wave in the Northern Hemisphere was lower during major SSW events of 2006 and 2009, compared with other undisturbed winters. Sassi et al. (2012) also attributed the reduced quasi-16-day wave activity during the winter of 2008–2009 to the occurrence of a major SSW. Luo et al. (2000) found no clear relationship between the quasi-16-day wave activity and SSWs in the wind data at 58- to 105-km altitude at Saskatoon (52°N, 107°W) during 1980–1996. Matthias et al. (2012), using mesospheric wind data from the meteor radar at Andenes (69°N, 16°E), performed a composite analysis for the wave response to SSW events in January 2004, 2006, 2009, and 2010. They showed that amplification occurs in the quasi-16-day and quasi-10-day waves before and after the polar vortex breakdown, respectively. Ma et al. (2017) and Xiong et al. (2018) observed enhanced quasi-2-day wave activity in the Northern Hemisphere during the SSW events of January 2013 and January 2017, respectively. Gu et al. (2018) ascribed enhanced $s = 2$

quasi-2-day wave activity during January–February 2006 to the occurrence of a major SSW in late January. Gong et al. (2018) observed an enhancement in the quasi-6-day wave amplitude at 80- to 100-km altitude during the January 2013 SSW event. Pancheva et al. (2018b) reported an enhancement in the quasi-6-day wave amplitude (not only for $s = 1$ but also for $s = 2$) during the January 2009 SSW event.

The present study examines long-period (3–20 days) waves in the middle atmosphere during November–May, when SSWs are most commonly observed. The focus is on westward propagating waves with zonal wave number $s = 1$, which includes the quasi-6-day wave, quasi-10-day wave, and quasi-16-day wave. As described in the previous paragraph, the response of these waves to SSWs is not well understood; meanwhile, for the response of the quasi-2-day wave to SSWs, there are dedicated studies in recent years (e.g., Gu et al., 2016, 2018). In previous studies, it was often difficult to distinguish the response of Rossby waves to SSWs from other transient variability of the waves. It is thus desirable to inspect as many SSW events as possible so that the repeatability of the SSW effect can be established. In this study, long-term (over 14 years) geopotential measurements from the Aura/Microwave Limb Sounder (MLS) are employed to determine the wave activity under different stratospheric conditions.

2. Data and Method of Analysis

2.1. Geopotential Height

The primary data used in this study are the geopotential height measurements from the MLS on the Aura satellite (Schwartz et al., 2008; Waters et al., 2006) during 2004–2018. Version 4.2 data (Livesey et al., 2017) were obtained from the Goddard Earth Sciences Data and Information Services Center (Acker & Leptoukh, 2007). The Aura/MLS measurements cover the latitude range of ±82° and the pressure levels from 261 (9 km) to 0.001 hPa (97 km). The pressure levels were converted to approximate heights, and in the remainder of this paper the results will be presented using these approximate heights.

The amplitude and phase of a wave with zonal wave number s and period τ can be evaluated by the least squares fitting of the following formula to the data:

$$A \cos\left[2\pi\left(\frac{t}{\tau} + s\lambda\right) - \phi\right], \tag{1}$$

where A is the amplitude of the wave, t is the universal time, λ is the longitude, and ϕ is the phase of the wave. Positive and negative values of s correspond to westward and eastward propagating waves, respectively. Before performing the fitting, the mean values were subtracted from the data, separately for the ascending and descending parts of the orbit. This largely avoids aliasing from the signals of migrating solar tides, because the Aura satellite is in a Sun-synchronous orbit and the ascending and descending parts of the orbit are stationary to the migrating solar tides (Meek & Manson, 2009). A and ϕ were computed at a given latitude, taking the measurements within ±5° from that latitude. The calculation was made for the waves with $s = 1$ and periods 3–20 days. The data were processed on each day using time windows that are 3 times the wave period. Similar time windows were previously used by Forbes et al. (2018) for the investigation of waves in a similar period range.

Yamazaki (2018) estimated uncertainties in the amplitude and phase of the quasi-6-day wave at 0.001 hPa (97 km) derived from the Aura/MLS geopotential height data. The same technique was applied here for the uncertainty estimates of the waves with various s and τ at various heights. The technique takes into account two sources of uncertainties. One is measurement errors and the other is fitting errors. The latter is due to the variance of the data points within the fitting window, which results from other natural variability unrelated to the wave of interest. The 1-σ uncertainties due to fitting errors can be estimated using the bootstrap technique (i.e., iterations of random resampling). The Aura/MLS data include estimates of measurement errors along with geopotential height values. The measurement errors depend mainly on the height; and according to the technical report by Livesey et al. (2017), typical values are ±20 m at 261–10 hPa (9–32 km), and ±25 m, ±45 m, ±110 m, and ±160 m at 1 hPa (48 km), 0.1 hPa (64 km), 0.01 hPa (81 km), and 0.001 hPa (97 km), respectively. In each bootstrap iteration, a random value was generated for each data point from the normal distribution that has the standard deviation of the size of the measurement error. These values (either positive or negative) were added to the data before the fitting is performed. In this way uncertainties due to measurement errors will propagate through the fitting formula (1). As noted by Yamazaki (2018), the fitting errors are usually greater than the measurement errors, and hence dominating the uncertainty estimates.

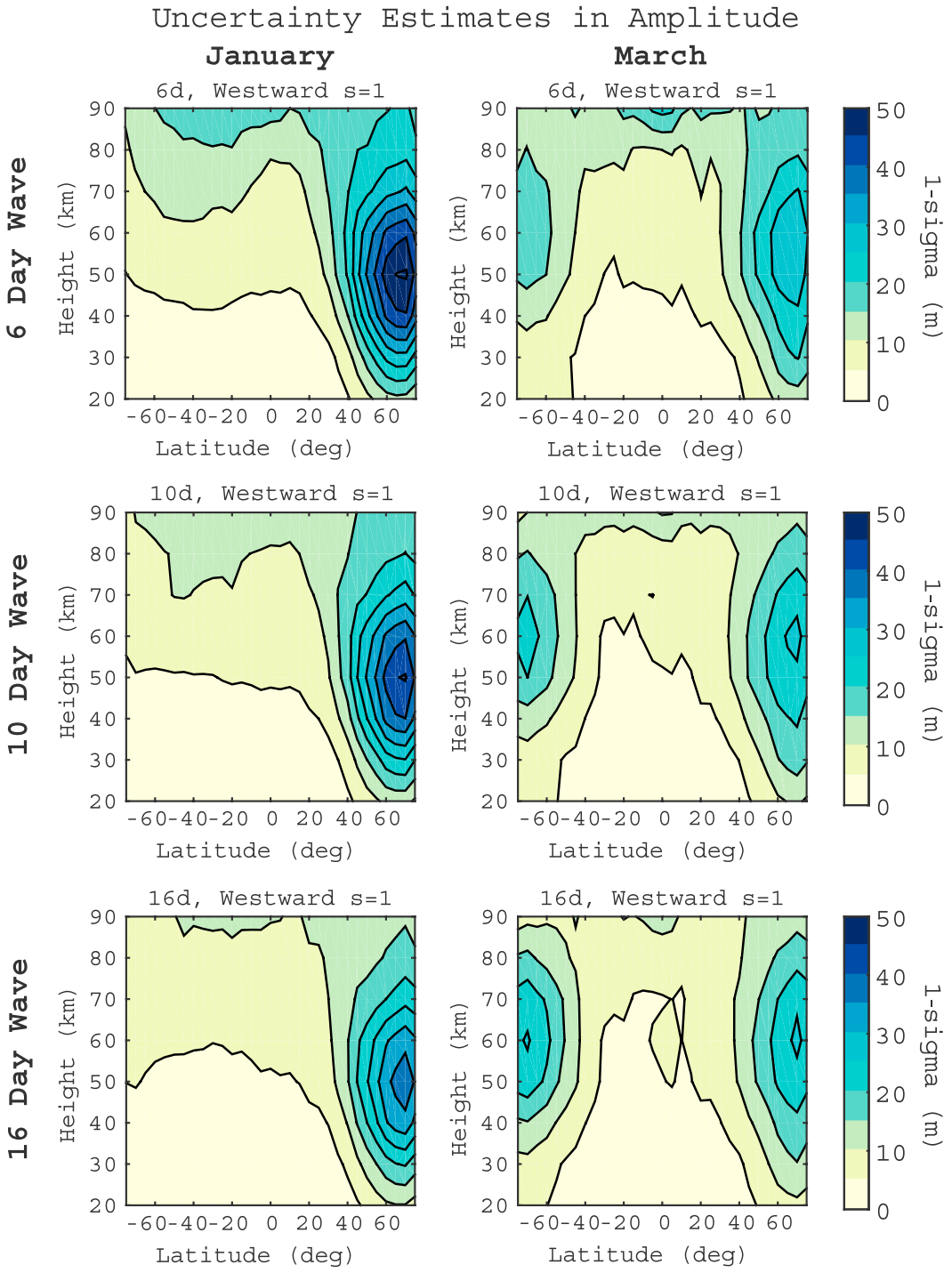

Figure 2. Mean 1-σ uncertainties in the wave amplitude. The top, middle, and bottom panels are for the westward propagating waves with Zonal Wave Number 1 at wave period 6, 10, and 16 days, respectively. The left and right panels are for January and March, respectively.

The mean values of the estimated 1-σ uncertainties in the amplitude (including contributions from both measurement errors and fitting errors) are presented in Figure 2 for January (left) and March (right). The top panels are for the westward propagating wave with zonal wave number $s = 1$ and period $\tau = 6$ days, while the middle and bottom panels are the same except for $\tau = 10$ days and $\tau = 16$ days, respectively. It can be seen that the uncertainty distribution depends on the season but not strongly so on the period of the

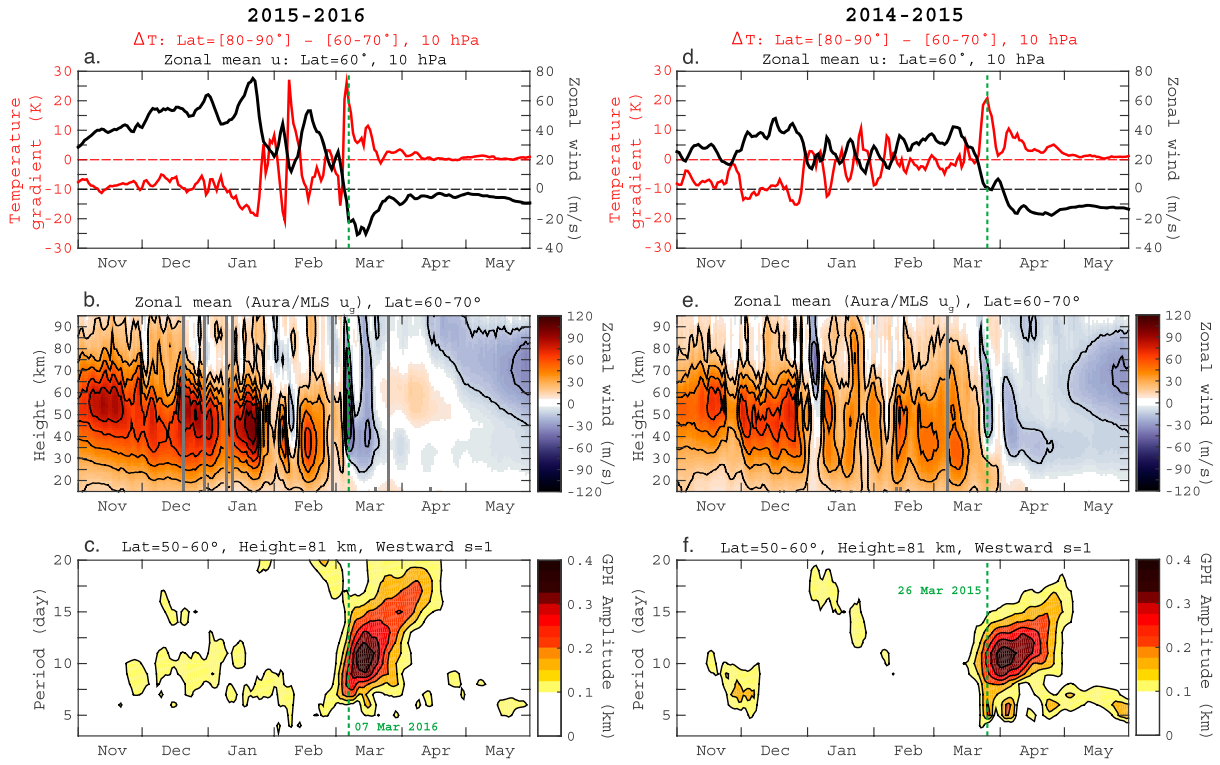

Figure 3. Examples of long-period (3–20 days) wave activity during the Northern Hemisphere winter and spring. (a, d) MERRA-2 meridional temperature gradient $\Delta T = \overline{T}(80–90°) – \overline{T}(60–70°)$ at 10 hPa and MERRA-2 zonal mean zonal wind at 60° latitude at 10 hPa. (b, e) Zonal mean of the Aura/MLS geostrophic zonal wind at 65° latitude. (c, f) Aura/MLS geopotential height (GPH) amplitudes of westward propagating waves with Zonal Wave Number 1 for wave period 3–20 days at 55° latitude and 81-km altitude. The day of the peak polar vortex weakening (i.e., minimum $\overline{u}_g$ at 1 hPa, 48 km) is indicated by the green vertical dashed line. The gray shaded areas in the middle and bottom panels indicate the times when there is no sufficient data. The left and right panels are for 2015–2016 and 2014–2015, respectively. MERRA-2 = Modern-Era Retrospective analysis for Research and Applications, Version 2; MLS = Microwave Limb Sounder.

wave. Relatively large values are seen at high latitudes in the winter hemisphere at 50- to 60-km altitude, probably reflecting large variability of the winter middle atmosphere. Day et al. (2011) also found highest fitting errors in the winter high latitudes in their investigation of the 16-day wave based on the Aura/MLS temperature data. As can be seen in Figure 2, the 1-σ uncertainty in the amplitude is generally less than 50 m. This is noticeably smaller than the amplitude of the waves discussed in this paper, which is typically in the range of 100–400 m.

2.2. Stratospheric Winds and Temperature

Daily mean values of the zonal mean zonal wind and temperature were obtained from the atmospheric reanalysis product, namely, Modern-Era Retrospective analysis for Research and Applications, Version 2 (MERRA-2; Gelaro et al., 2017). The data were used to identify SSW events. The identification of SSW events is based on the breakdown of the polar vortex and the reversal of the meridional temperature gradient in the high-latitude region. The polar vortex breakdown is defined by the reversal of the zonal mean zonal wind at 60° latitude at 10 hPa (32 km), while the meridional temperature gradient reversal is defined as the zonal mean temperatures averaged from 80°N to 90°N at 10 hPa minus the temperatures averaged from 60°N to 70°N at 10 hPa. This is one of the most commonly used procedures for detecting major SSWs (Butler et al., 2015), and it has been used in previous studies on the response of atmospheric waves to SSWs in the middle atmosphere (e.g., Matthias et al., 2012; Sridharan et al., 2009). Events are called minor if the temperature gradient reversal is observed without a reversal of the zonal mean flow at 60° latitude at 10 hPa. Also, events are considered to be final warmings if the zonal mean flow does not change back eastward for at least 10 consecutive days before 30 April.

A major SSW rarely occurs in the Southern Hemisphere (e.g., Krüger et al., 2005), and in fact, there was no major Antarctic SSW event during the period of investigation. The scope of this study is, thus, limited to the SSW events in the Northern Hemisphere.

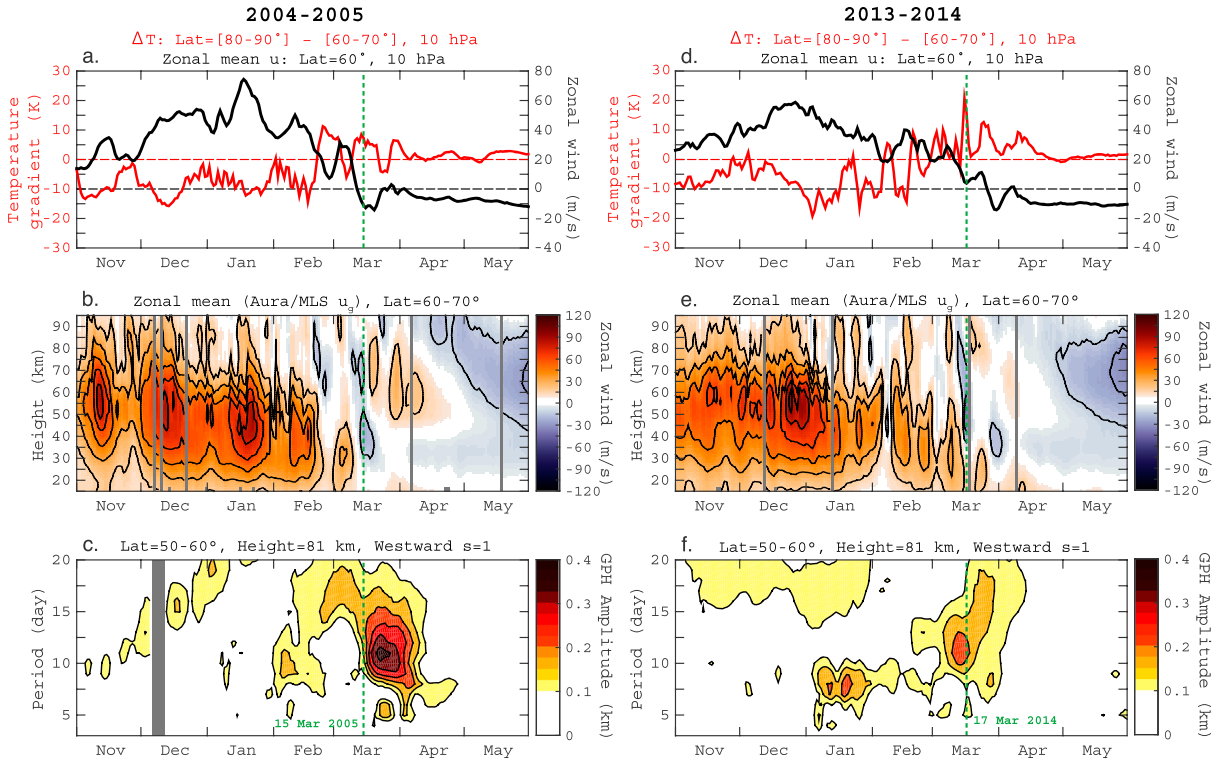

Figure 4. Same as Figure 3 except for 2004–2005 (a–c) and 2013–2014 (d–f).

The geostrophic winds were derived from the Aura/MLS geopotential height data using the method described by Matthias and Ern (2018). The zonal mean of the zonal geostrophic wind, $\overline{u}_g$, is used to observe the zonal mean state of the middle atmosphere beyond the height limit of MERRA-2 (up to 0.1 hPa, 64 km). $\overline{u}_g$ is also used to determine the central day of SSWs. More specifically, the day of "peak polar vortex weakening" is defined to be when $\overline{u}_g$ at 60–70° latitude at 1 hPa (48 km) reaches its minimum value during November–April of each year. The peak polar vortex weakening at 1 hPa has been used as the central day of SSWs in previous studies on the middle/upper atmosphere response to SSWs (e.g., Chau et al., 2015; Siddiqui et al., 2015; Yamazaki et al., 2015; Zhang & Forbes, 2014). There is generally good agreement between the days of peak polar vortex weakening determined by $\overline{u}_g$ and by the MERRA-2 zonal wind at 1 hPa.

3. Results

Figure 3a displays the zonal mean zonal wind (black) and temperature gradient (red) at 10 hPa (32 km) during the months November–May of 2015–2016, as derived from the MERRA-2 data. Figure 3b shows the height structure of the zonal mean zonal wind $\overline{u}_g$ at 60–70° latitude, derived from the Aura/MLS measurements, and Figure 3c shows the amplitude of westward propagating $s = 1$ waves at 55° latitude at 0.01 hPa (81 km) for wave periods ranging 3–20 days. The vertical dashed lines indicate the day of the peak polar vortex weakening, which was defined in the previous section.

As shown in Figure 3a, there is no major SSW from November 2015 to February 2016. Studies showed that the polar vortex was unusually strong and cold during December 2015–January 2016 (e.g., Matthias et al., 2016; Stober et al., 2017). Three minor SSW events occurred from late January to February 2016, where the temperature gradient became positive but the zonal mean zonal wind did not fall below 0 m/s. The polar vortex breakdown occurred in early March 2016, as indicated by a rapid decrease in the zonal mean zonal wind below 0. The reversal of the zonal mean flow is seen to extend from the stratosphere ~30 km to the lower thermosphere >90 km (Figure 3b). The event is categorized as a final warming, because the zonal mean zonal wind at 60° latitude at 10 hPa (Figure 3a) did not go back to a positive value until the following winter. As seen in Figure 3c, the polar vortex breakdown was accompanied by a sudden increase in the

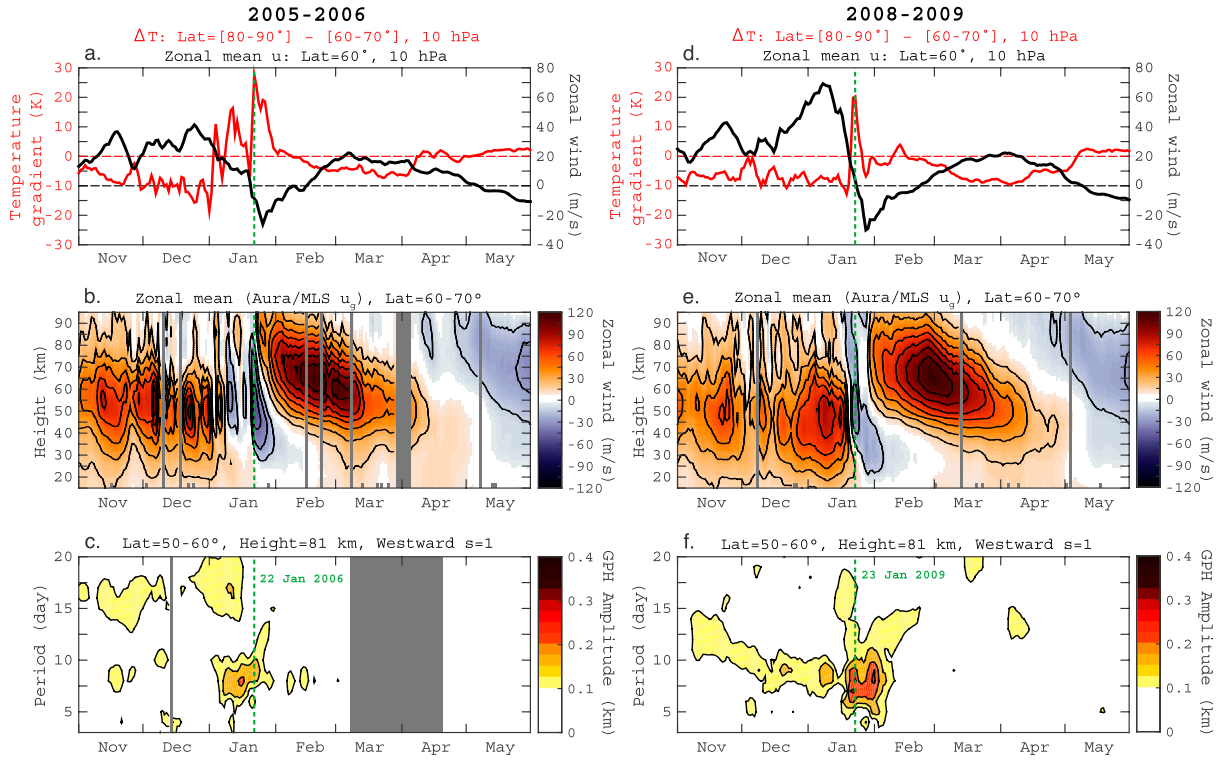

Figure 5. Same as Figure 3 except for 2005–2006 (a–c) and 2008–2009 (d–f).

amplitude of westward propagating $s = 1$ waves at period 7–18 days. It appears that the enhanced wave activity occurs first for shorter-period waves then later for longer-period waves. The largest amplitude is found at period τ ~10 days.

Figures 3d and 3e reveal a series of minor warmings in January–February 2015. Toward the end of March 2015, there was a rapid decrease in the zonal mean zonal wind, accompanied by a sharp increase in the temperature gradient to positive values. The zonal mean zonal wind at 60° latitude at 10 hPa went below 0 on 28 March 2015, signifying the reversal of the stratospheric polar jet. Although there was a brief period of eastward zonal wind during 29 March to 2 April 2015, the reestablishment of the eastward jet did not occur until the following winter, which makes this SSW event a final warming.

The response of westward propagating $s = 1$ waves during this final warming event is depicted in Figure 3f. Similar to the March 2016 case (Figure 3c), enhanced wave activity is observed following the peak polar vortex weakening at 1 hPa (48 km) on 26 March 2015. A large-amplitude wave is first seen at period $\tau = 5$–6 days, then around $\tau = 10$ days, and later at longer periods. Relatively high wave activity at period $\tau = 5$–6 days is visible intermittently until the end of May.

One common feature in the stratospheric dynamics during November–May of 2015–2016 (Figures 3a– 3c) and 2014–2015 (Figures 3d– 3f) is that in both cases, there was no major "midwinter" SSW event. That is, the zonal mean zonal wind at 60° latitude at 10 hPa stayed positive until the spring transition that was accompanied by a final warming. Figure 4 shows two other cases where there was no reversal of the zonal mean flow during November–February. The same parameters are presented in Figure 4 as in Figure 3 but for 2004–2005 (left) and 2013–2014 (right).

In Figure 4a, the reversal of the zonal mean zonal wind at 10 hPa is seen on 12 March 2005, accompanied by a temperature gradient reversal. After the peak polar vortex weakening at 1 hPa (48 km) on 15 March 2005, the zonal mean flow returned eastward in the mesosphere at 50–80 km (Figure 4b), but in the stratosphere (at 10 hPa, 32 km), the eastward jet did not fully recover by the end of April, which makes this event a final warming. There was enhanced westward propagating $s = 1$ wave activity at 55° latitude following the peak polar vortex weakening at 1 hPa, which is similar to the March 2016 and April 2015 cases. The largest amplitude is seen at period τ ~10 days. There is also a separate peak at period τ ~5 days, which is similar to

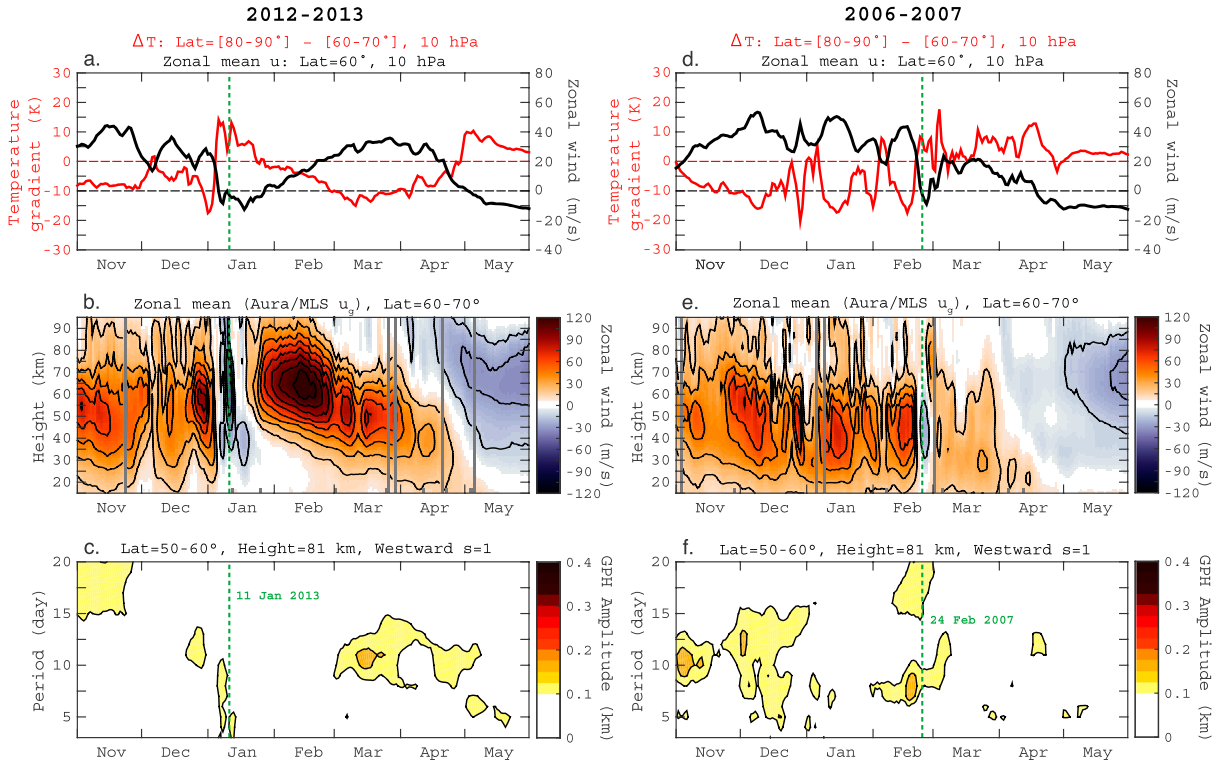

Figure 6. Same as Figure 3 except for 2012–2013 (a–c) and 2006–2007 (d–f).

the April 2015 case (Figure 3f). In contrast to the 2016 and 2015 cases, enhanced wave activity is first seen for long-period waves τ = 15–20 days, then later at shorter periods. The reason for this is unclear.

No major SSW event was recorded during November 2013–February 2014 (Figures 4d– 4f). The peak polar vortex weakening on 17 March 2014 corresponds to a minor warming where the stratospheric polar jet does not reverse westward. Relatively large waves at period τ = 10–13 days are observed during 10–16 March 2014, before the peak polar vortex weakening. Also, wave activity is seen at period τ = 7–9 in January 2014 (Figure 4f) without a major SSW event.

Figure 5 shows two cases, where there is a major SSW event in January. The left panels are for the winter 2005–2006, and the right panels are for the winter 2008–2009. The SSW events of January 2006 and 2009 have been documented as intense long-lasting SSWs Manney et al. (2008, 2009).

As seen in Figures 5a and 5b, the stratosphere was markedly disturbed during January 2006. The zonal wind reversal at 10 hPa was recorded on 21 January 2006 (i.e., major warming) after a couple of minor warmings. The peak polar vortex weakening at 1 hPa (48 km) occurred on 22 January 2006, coinciding with the peak in the temperature gradient. Figure 5c reveals that westward propagating s = 1 waves were relatively enhanced at period τ ~8 days in mid-January, when the zonal mean flow was westward at 40–70 km (Figure 5b).

The spring transition occurred on 7 May 2006, as determined by the zonal mean zonal wind at 60° latitude at 10 hPa (32 km). This is rather late compared to the other years examined above (i.e., 2016, 2015, 2005, and 2014). Hu et al. (2014) pointed out that the spring transition generally occurs later when there is an SSW event in the preceding winter. No distinct Rossby wave activity is seen in Figure 5c around the spring transition of 2006.

Figures 5d and 5e depict a rapid breakdown of the stratospheric polar vortex with a sharp rise and reversal in the temperature gradient during the January 2009 major SSW event. The peak polar vortex weakening at 1 hPa (48 km) occurred on 23 January 2009. Enhanced wave activity is seen in Figure 5f from 20 January until early February 2009 at period τ = 6–10 days. This is followed by an extended period of low wave activity until the end of May 2009. Similar to 2006, the spring transition occurred late on 3 May 2009 with no distinct Rossby wave activity.

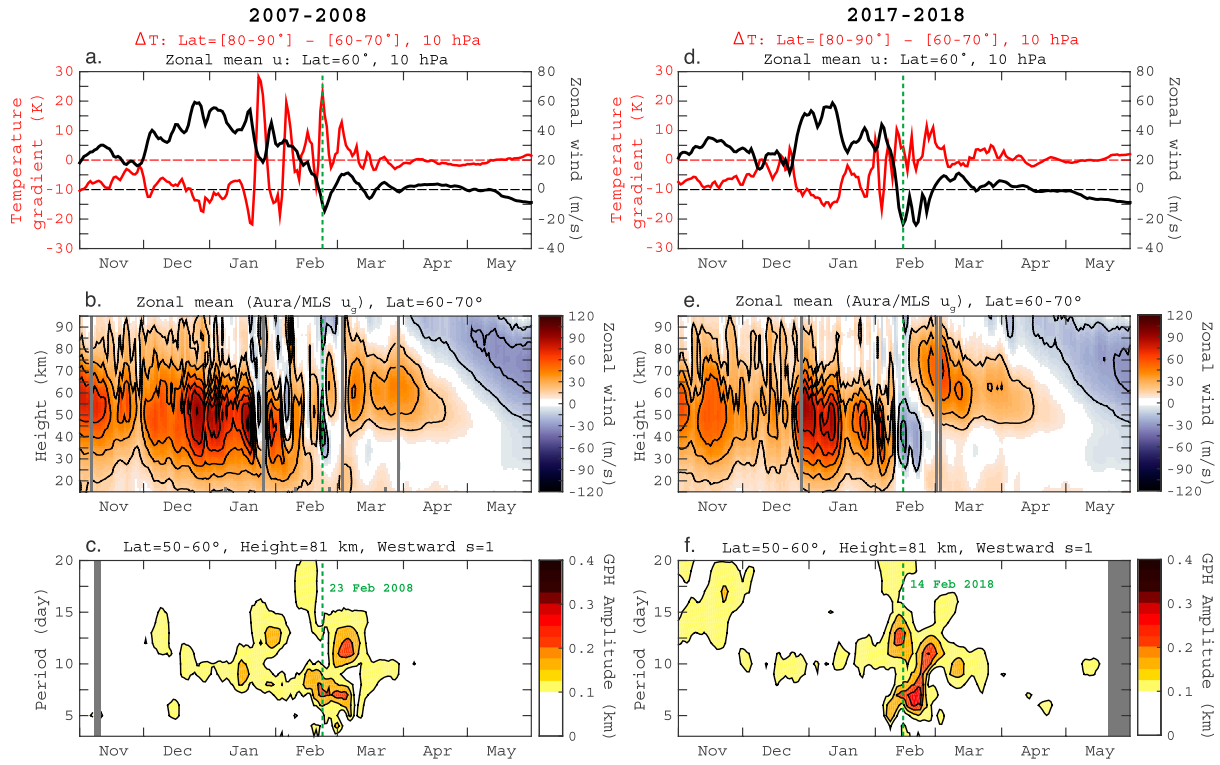

Figure 7. Same as Figure 3 except for 2007–2008 (a–c) and 2017–2018 (d–f).

Two other examples of major SSW events are given in Figure 6. The left panels are for the January 2013 SSW event and the right panels are for the February 2007 SSW event. In both cases, no clear SSW response is detected in westward propagating $s = 1$ waves at 55° latitude at 81-km altitude (Figures 6c and 6f). The spring transition occurred on 2 May 2013 and 10 April 2007 as a smooth process, again, without a final warming or distinct Rossby wave activity in the mesosphere.

Figure 7 presents two more examples of major SSW events. The February 2008 SSW event, shown in the left panels, is characterized by large oscillations in the temperature gradient (Figure 7a) and zonal mean flow at ~50 km (Figure 7b), which started around 20 January 2008. Following the peak polar vortex weakening on 23 February 2008, enhanced wave activity is observed at period τ ~7 days and also at τ = 11–13 days, which continues until early March. The wave response is similar during the 2018 SSW event (Figures 7d– 7f). After the peak polar vortex weakening on 14 February 2018, there is enhanced wave activity at period τ ~7 days and τ ~11 days.

In summary, we found strong transient Rossby wave activity starting at final warmings with periods of τ ~5–20 days. Also, there is sometimes an increase in transient Rossby wave activity around midwinter SSWs with periods of τ ~5–16 days but with much smaller magnitudes compared to final warmings, and response characteristics (e.g., peak period) vary from event to event. Results from other latitudes and heights (not shown here) also did not reveal any consistent response to midwinter SSWs. The winters in which a midwinter SSW occurred are coincided with a smooth spring transition and thus without a final warming and without increased transient Rossby wave activity. In the following we will discuss the unusually strong transient Rossby wave activity starting at final warmings in more detail.

4. Discussion

Westward propagating $s = 1$ waves with particularly large amplitudes are observed at 55° latitude at 81-km altitude in March 2016, April 2015, and March 2005, following the final breakdown of the stratospheric polar vortex. Associated disturbances are clearly visible in Figure 8, which depicts the deviation of the geopotential height from the seasonal mean. In each case, westward propagating perturbations with oscillation period about 10 days lasted for two to three wave cycles. This section focuses on these extraordinary events and

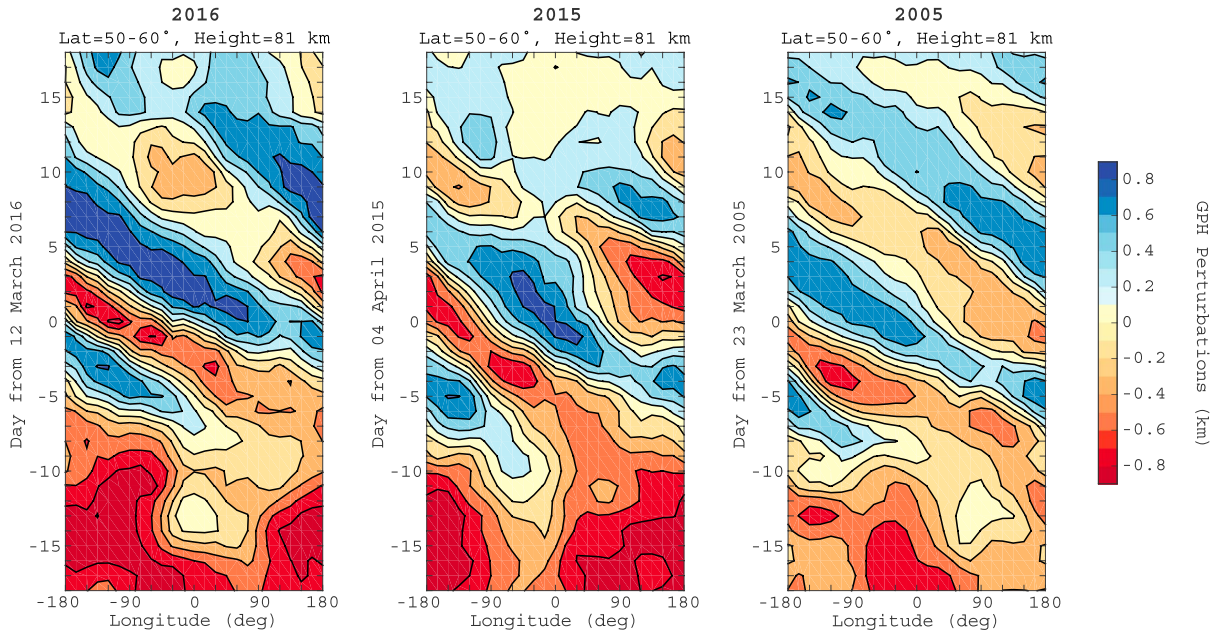

Figure 8. Aura/Microwave Limb Sounder geopotential height (GPH) variations from the seasonal mean at 55° latitude and 81-km altitude. The vertical axis presents time in days from 12 March 2016 (left), 4 April 2015 (middle), and 23 March 2005 (right).

describes their characteristics in detail. The most likely candidate for the observed large-amplitude waves is the second antisymmetric Rossby normal mode (1,2), or the quasi-10-day wave, for their zonal wave number and wave period. For convenience, this interpretation is adopted from now on and observed waves with $s = 1$ and $\tau \sim 10$ days are referred to as the quasi-10-day wave. As will be shown later, the horizontal and vertical structures of the waves observed in March 2016, April 2015, and March 2005 are also consistent with the quasi-10-day wave.

Figure 9 displays time series of the quasi-10-day wave amplitude at 55° latitude at 15- to 95-km altitude (top). The amplitude is taken to be the largest value from the least squares fitting for wave periods between 8.5 and 11.5 days. Figure 9 also shows the waves with $s = -1$ (upper middle), $s = 2$ (lower middle), $s = -2$ (bottom) for the same period range. As stated earlier, positive and negative wave numbers signify westward and eastward propagations, respectively. In Figure 9, the occurrence times of peak polar vortex weakening are also indicated for winter/spring months (November–April) of each year, along with the type of the corresponding SSW event (major, minor, or final). The following features are seen in Figure 9: (1) the westward propagating $s = 1$ wave is usually dominant but sometimes the eastward propagating $s = -1$ is comparable or even larger; (2) the waves with Zonal Wave Number 2 are usually smaller than the waves with Zonal Wave Number 1; and (3) the wave amplitude tends to be larger in winter than in summer regardless of wave number. These features are in agreement with earlier studies (e.g., John & Kumar, 2016). Wave amplitudes are sometimes comparable between $s = 1$ and $s = -1$ (e.g., December 2005) and also sometimes between $s = 2$ and $s = -2$. These wave signals are in part due to the temporal variability of stationary planetary waves. A stationary planetary wave, $A\cos\left(2\pi\frac{t}{\tau}\right)\cos(2\pi s\lambda)$, can also be expressed as $\frac{A}{2}\cos\left[2\pi\left(\frac{t}{\tau}+s\lambda\right)\right] + \frac{A}{2}\cos\left[2\pi\left(\frac{t}{\tau}-s\lambda\right)\right]$ and thus is equivalent to two oppositely propagating waves with equal amplitudes, periods, and wave numbers.

During the final warmings of March 2016, 2015, and 2005, large-amplitude quasi-10-day waves are observed around the stratopause height (~48 km) and above. No corresponding wave activity is found in $s = -1$, $s = 2$, and $s = -2$. There is another final warming event in April 2011; however, the geopotential height data are missing during this event. Large-amplitude quasi-10-day waves are also observed at lower heights (40–60 km) during January 2008 and 2011. A closer inspection of the data revealed that the peak period is $\tau \sim 12$–13 days in both cases. Although there are minor SSWs during January 2008 and 2011, the link to the wave activity was unclear and thus these events will not be further investigated here.

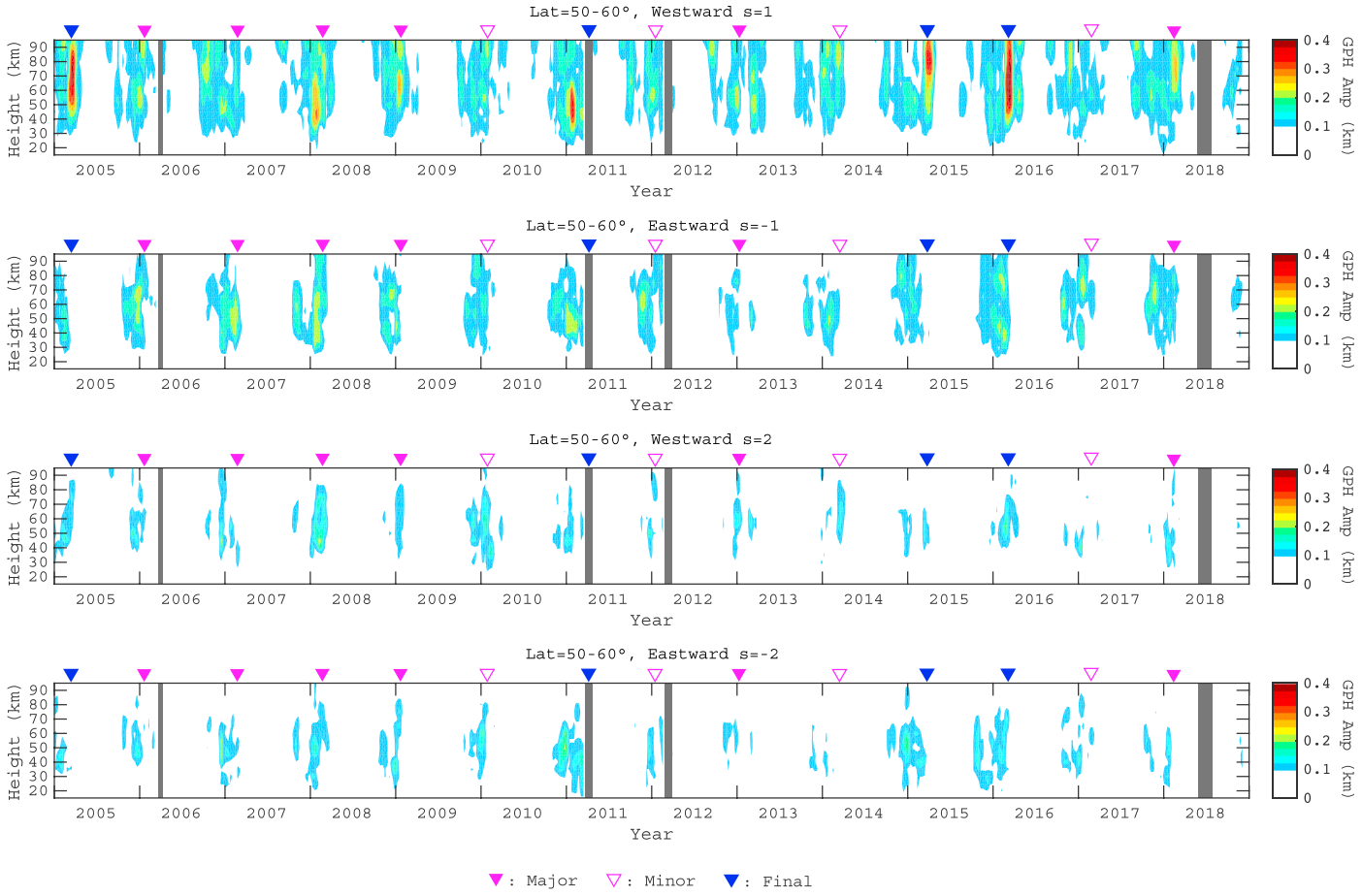

Figure 9. Height versus time distributions of the amplitude of waves with period near 10 days (i.e., the maximum amplitude between τ = 8.5 and 11.5 days) at 55° latitude during 2004–2018. The top and upper middle panels are for the westward and eastward propagating waves with Zonal Wave Number 1, respectively. The lower middle and bottom panels are for the westward and eastward propagating waves with Zonal Wave Number 2, respectively. The occurrence of the peak polar vortex weakening at 1 hPa (48 km) is indicated for each year during November–April, along with the type of the corresponding SSW event (major, minor, or final). GPH = geopotential height.

Figure 10 shows the quasi-10-day wave amplitude at various heights during the 2016 event (left), 2015 event (middle), and 2005 event (right). Also plotted in each panel is the corresponding climatological seasonal cycle of the quasi-10-day wave amplitude with its standard deviation, which was derived using the data for 2005–2018 but excluding the times of large-amplitude quasi-10-day wave events, defined here as ±15 days from 12 March 2016, 4 April 2015, and 23 March 2005. Significant enhancement in the quasi-10-day wave amplitude can be seen at the stratopause height (48 km) and above around 12 March 2016, 4 April 2015, and 23 March 2005. During these events, the amplitude of the quasi-10-day wave was ~0.4 km at the mesopause height (81 km), which is approximately 4 times the climatological value of ~0.1 km. There is no evidence for enhanced quasi-10-day wave activity at 32 km and below. Thus, the amplification or excitation of the quasi-10-day wave probably occurred in the upper stratosphere, approximately 30–50 km.

Figure 11 shows the horizontal and vertical structures of the westward propagating wave with zonal wave number s = 1 and period τ = 10 days for ±15 days from 12 March 2016 (left), 4 April 2015 (middle), and 23 March 2005 (right). The amplitude and phase were calculated at wave period of exactly 10.0 days, so that the phases derived at different heights and latitudes can be compared. It may be noted in Figures 11a– 11c that the amplitude structures are similar for the March 2016 event and March 2005 event. That is, in both cases the amplitude peaks at 55–60° latitude at 65- to 70-km altitude in the Northern Hemisphere, and the amplitude in the Southern Hemisphere is mostly below 0.1 km. For the April 2015 event, on the other hand, the amplitude distribution is more symmetric about the equator, and there are amplitude maxima around ±55° latitude. Also, the amplitude peak in the Northern Hemisphere is seen at a higher altitude ~81 km

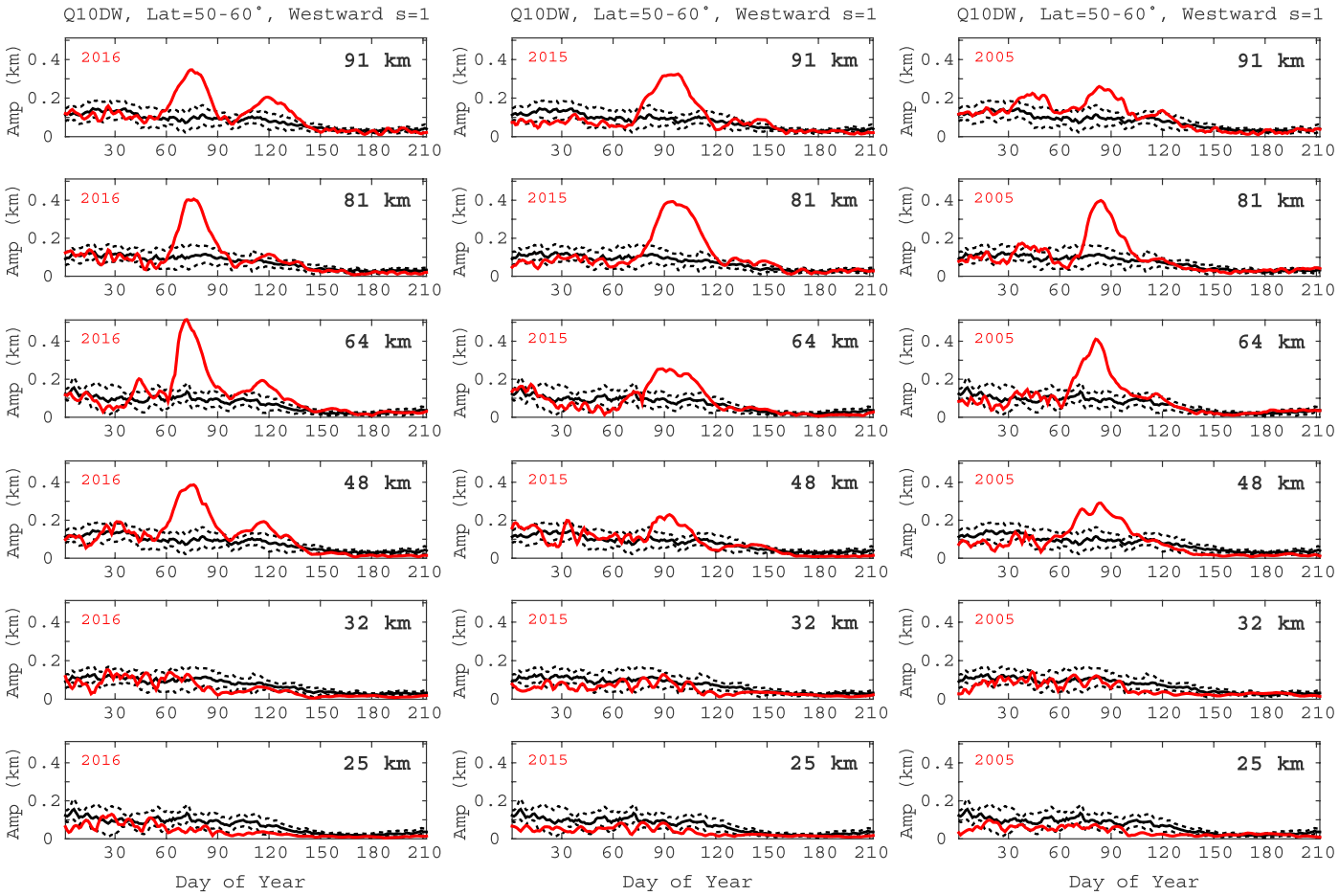

Figure 10. Quasi-10-day wave (Q10DW) amplitude in geopotential height at, from the top to the bottom, 91-, 81-, 64-, 48-, 32-, and 25-km altitudes for 2016 (left), 2015 (middle), and 2005 (right). In each panel the black solid line indicates the corresponding climatological seasonal cycle and the black dashed lines represent its standard deviation.

compared with the March 2016 and March 2005 events. Nevertheless, the overall latitudinal structures of the amplitude presented in Figures 11a– 11c are consistent with the Rossby normal mode (1,2), which has the amplitude maxima at ±55° latitude (see Figure 1). According to the modeling study by Salby (1981b), the amplitude distribution is symmetric about the equator under equinoctial conditions, while under solstitial conditions the amplitude is much greater in the winter hemisphere than in the summer hemisphere. Thus, the April 2015 event (Figure 11b) represents the equinoctial type, while the March 2016 and March 2005 events represent the solstitial type (although the March 2005 event is closest to the equinox).

Figures 11a– 11c also depict the height profiles of the phase in the Northern Hemisphere at 55° latitude. The calculation of the phase is limited to the height range where the amplitude is larger than 0.1 km. For the April 2015 event (middle), the height profile of the phase is also shown for the Southern Hemisphere at −55° latitude. The phase profiles reveal a westward tilt in all cases, indicating upward energy propagation. A fit of a straight line to the phase values within the height range shown in Figures 11a–11c indicates the estimated vertical wavelength of 111, 96, and 146 km for the March 2016, April 2015, and March 2005 events, respectively. Forbes and Zhang (2015), in their survey of the average quasi-10-day wave during 2002–2013, found a similar vertical phase tilt. In classical wave theory, the vertical structure of the normal mode Rossby waves is the same as that of the Lamb wave, which has an infinite vertical wavelength (and hence no vertical phase change), in the absence of dissipation and nonuniform background. The vertical phase tilt can arise from the inclusion of dissipation (e.g., Salby, 1980) and mean winds (e.g., Salby, 1981a). Thus, the phase variation with height does not necessarily conflict with the normal mode interpretation. In Figure 11b, a westward tilt in the phase is seen in the Southern Hemisphere as well as in the Northern Hemisphere. The 10-day waves at ±55° latitude are approximately 180° out of phase, which is consistent with the antisymmetric (1,2) mode.

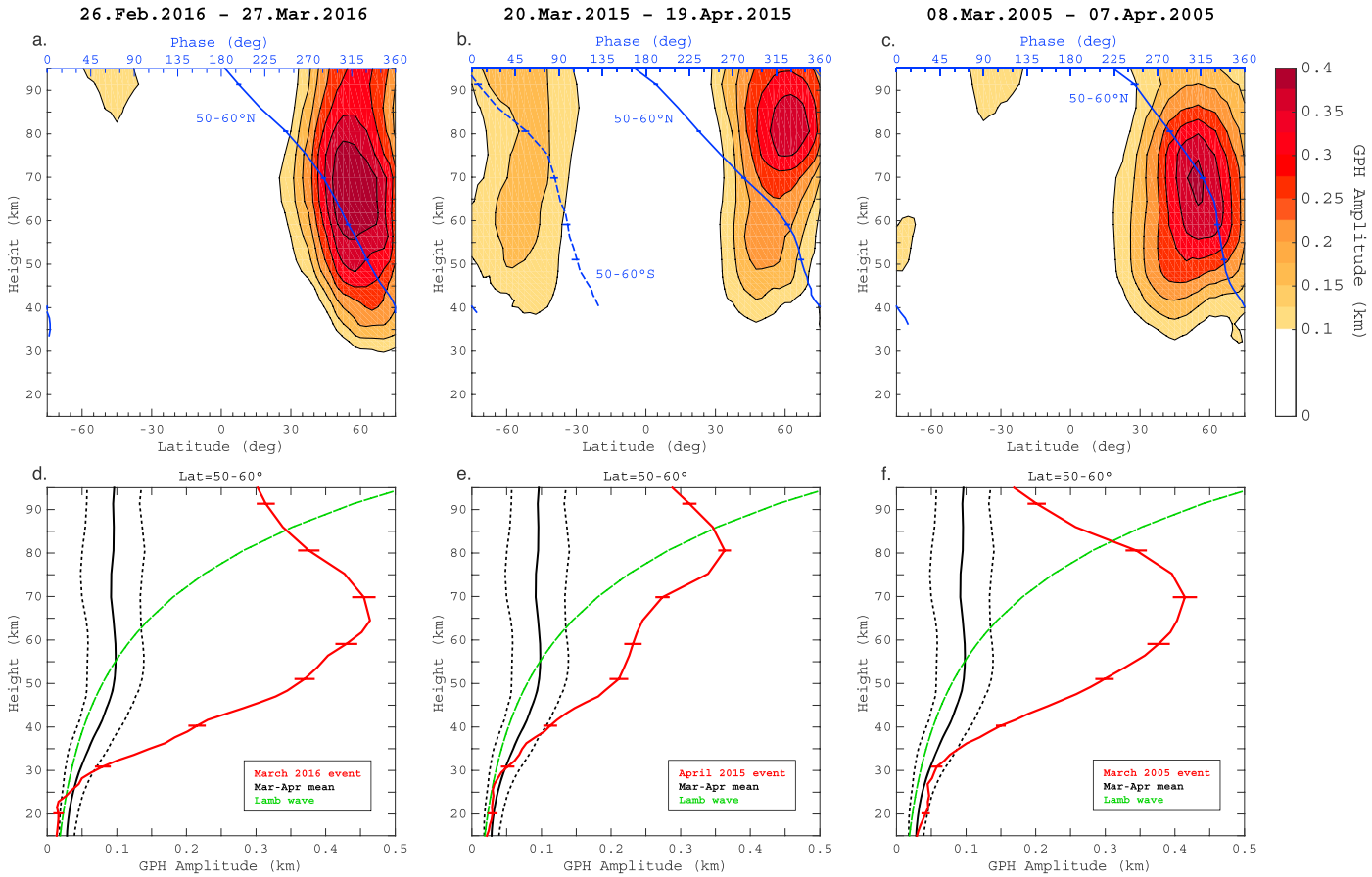

Figure 11. Latitude versus height structures of the westward propagating 10-day wave with Zonal Wave Number 1 on 12 March 2016 (a, d), 4 April 2015 (b, e), and 23 March 2005 (c, f). The (a–c) 10-day wave amplitude in geopotential height (GPH) and phase at 55° latitude. (d–f) Amplitude profile of the observed 10-day wave at 55° latitude, along with the theoretically predicted amplitude profile for Rossby normal modes, namely, $\exp(\kappa z/H)$, where κ=0.29, z is the altitude, and H is the scale height. Also shown is the amplitude profile of the seasonal mean quasi-10-day wave (March–April) with its standard deviation.

Figures 11d–11f show the vertical profiles of the 10-day wave amplitude at 55° latitude during the March 2016, April 2015, and March 2005 events. Also shown are the amplitude profile of the seasonal mean quasi-10-day wave (March–April) and the height dependence of the Lamb wave, which is given by $\exp(\kappa z/H)$ where κ=0.29, z is the altitude, and H is the scale height. The vertical growth of the seasonal mean quasi-10-day wave is in agreement with that of the Lamb wave in the stratosphere (10–50 km), but in the mesosphere (>50 km), the wave growth is restricted and the amplitude is nearly constant with height. Similar results were reported by Hirooka (2000) for the quasi-10-day wave observed by the Upper Atmosphere Research Satellite during May 1992. During the March 2016, April 2015, and March 2005 events, the amplitude profiles largely deviate from the classical normal mode behavior as well as from the seasonal mean. The vertical growth rate is significantly greater than the theoretical predictions in the upper stratosphere (approximately 30–50 km). The results suggest the amplification or excitation of the quasi-10-day wave in that region, which is in line with the conclusion derived from Figure 10.

Studies have shown that normal mode Rossby waves can be generated by barotropic/baroclinic instabilities, where the potential vorticity has a negative meridional gradient (e.g., Lieberman et al., 2003; Salby & Callaghan, 2001; Sato & Nomoto, 2015). The necessary condition for the barotropic/baroclinic instability is $\mathrm{d}\overline{Q}/\mathrm{d}\phi < 0$, where $\mathrm{d}\overline{Q}/\mathrm{d}\phi$ is the meridional gradient of the quasi-geostrophic potential vorticity:

$$\frac{\mathrm{d}\overline{Q}}{\mathrm{d}\phi} = \frac{2\Omega\cos\phi}{a} - \frac{1}{a^2}\frac{\partial}{\partial\phi}\left[\frac{1}{\cos\phi}\frac{\partial}{\partial\phi}\left(\overline{u}_g\cos\phi\right)\right] - \frac{1}{\rho}\frac{\partial}{\partial z}\left(\rho\frac{f^2}{N^2}\frac{\partial\overline{u}_g}{\partial z}\right). \quad (2)$$

Here ϕ is latitude, z is height, Ω is the rotation rate of the Earth ($=2\pi\mathrm{d}^{-1}$), a is the Earth's radius, f is the Coriolis parameter, N is the buoyancy frequency, and ρ is the air density. Figure 12 shows the latitude

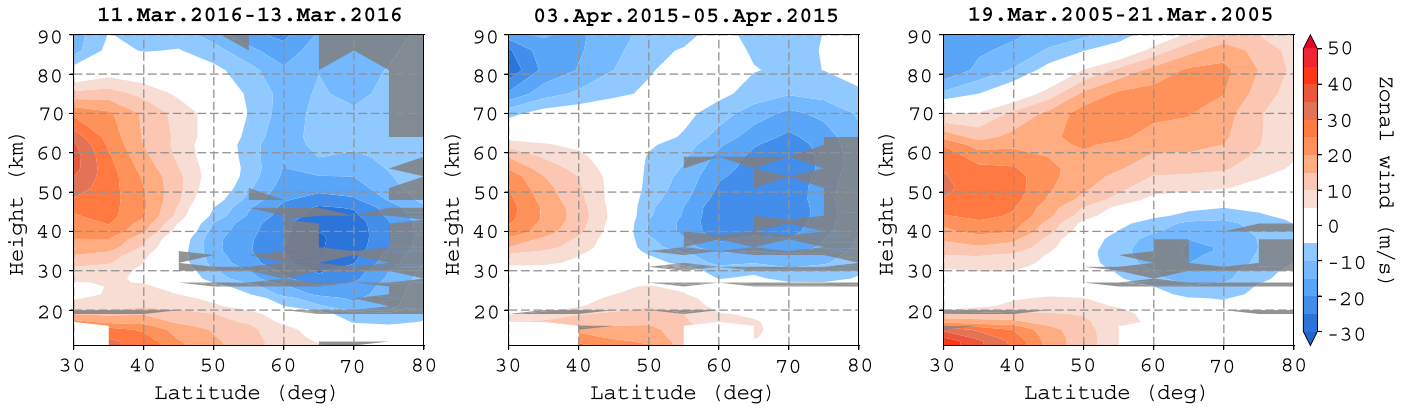

Figure 12. Latitude versus height structures of the zonal mean zonal wind $\overline{u}_g$ averaged over 3 days around 12 March 2016 (left), 4 April 2015 (middle), 20 March 2005 (right). The gray shaded areas indicate the regions where the necessary condition for the barotropic/baroclinic instability is met ($d\overline{Q}/d\phi < 0$).

versus height structures of the zonal mean zonal wind in the Northern Hemisphere when the large-amplitude quasi-10-day waves are observed. In the same figure, the gray shaded areas indicate the regions where the instability condition is satisfied ($d\overline{Q}/d\phi < 0$). At 50–60° latitude, the unstable regions are seen at 25- to 35-km altitude, which is just below the regions of rapid wave growth (see Figures 11d– 11f). For the April 2015 event, an unstable region also exists at higher altitudes 55–60 km. This is consistent with the two-step growth of the wave shown in Figure 11e. These results suggest the possibility that the observed large-amplitude quasi-10-day waves are generated by barotropic/baroclinic instability.

Further work is required to clarify the mechanism. Especially, simulations and numerical experiments based on models that include coupling processes from the surface to the middle and upper atmosphere would be useful to provide insight into how the occurrence of final warmings alters the source, propagation, and dissipation of the quasi-10-day wave.

5. Summary and Conclusions

Despite many studies in the past, the influence of SSWs on Rossby normal modes is not well understood. The present study utilizes over 14 years of geopotential height measurements from the Aura satellite to investigate the SSW effect on long-period waves (τ = 3–20 days), in particular, those propagate westward with zonal wave number $s = 1$, including the quasi-6-day wave, quasi-10-day wave, and quasi-16-day wave.

Enhanced wave activity is observed near wave period $\tau = 10$ days at 55° latitude between 48- and 97-km altitudes, following the final breakdown of the stratospheric polar vortex of 2016, 2015, and 2005 (Figures 3 and 4). Wave activity with similarly large amplitude is not observed during midwinter SSWs (Figures 5– 7) or during normal spring transitions where the breakdown of the polar vortex takes place slowly. The results suggest that not only the occurrence of SSW but also the seasonal timing of SSW is important for the wave variability in the middle atmosphere.

The large-amplitude waves observed in March 2016, April 2015, and March 2005 are interpreted to be the quasi-10-day wave, or the second antisymmetric Rossby normal mode (1,2) of Zonal Wave Number 1. The latitude and height structures of the waves are consistent with the quasi-10-day wave in the presence of dissipation and nonuniform background. The peak amplitudes are observed at 55–60° latitude (Figures 11). The vertical profile of the phase reveals a westward tilt (Figure 11), which is a characteristic of an upward propagating wave. The estimated vertical wavelengths are 111, 96, and 146 km for the March 2016, April 2015, and March 2005 events, respectively. The waves at ±55° latitude are approximately 180° out of phase, as shown for the April 2015 event.

The vertical growth rate of the amplitude in the upper stratosphere (approximately 30–50 km) is significantly greater than the classical normal mode, which is proportional to $\exp(\kappa z/H)$. Thus, the waves are likely amplified or excited in that region. The barotropic/baroclinic instability is suggested as a possible mechanism to generate the waves. Unstable regions (where $d\overline{Q}/d\phi < 0$) are found just below the regions of rapid wave growth (Figure 12). As a result of rapid wave growth in the stratosphere, the wave amplitudes at the

mesopause height (81 km) are much larger than in other years. More specifically, the quasi-10-day wave amplitudes during the March 2016, April 2015, and March 2005 events are approximately 4 times the climatological seasonal values derived from the data of other years (Figure 10 and 11). In each case, enhanced wave activity is observed for the duration of two to three wave cycles (Figure 8).

Finally, the present study mainly focused on the Northern Hemisphere. The variability of Rossby normal modes in the Southern Hemisphere and its relationship to Antarctic SSWs remains to be investigated.

Acknowledgments
The author thanks the NASA Goddard Earth Sciences (GES) Data and Information Services Center (DISC; https://disc.gsfc.nasa.gov/) for making the Aura/MLS geopotential height data and MERRA-2 data available. This work was supported in part by the Alexander von Humboldt Foundation and the Deutsche Forschungsgemeinschaft (DFG) Grant YA-574-3-1. Open access funding enabled and organized by Projekt DEAL.

References

Acker, J. G., & Leptoukh, G. (2007). Online analysis enhances use of NASA Earth science data. *Eos, Transactions American Geophysical Union*, *88*(2), 14–17.

Andrews, D. G., Leovy, C. B., & Holton, J. R. (1987). *Middle atmosphere dynamics* (Vol. 40). New York: Academic Press.

Burks, D., & Leovy, C. (1986). Planetary waves near the mesospheric easterly jet. *Geophysical Research Letters*, *13*(3), 193–196.

Butler, A. H., Seidel, D. J., Hardiman, S. C., Butchart, N., Birner, T., & Match, A. (2015). Defining sudden stratospheric warmings. *Bulletin of the American Meteorological Society*, *96*(11), 1913–1928.

Chang, L. C., Palo, S. E., & Liu, H.-L. (2011). Short-term variability in the migrating diurnal tide caused by interactions with the quasi 2 day wave. *Journal of Geophysical Research*, *116*, D12112. https://doi.org/10.1029/2010JD014996

Chau, J., Hoffmann, P., Pedatella, N., Matthias, V., & Stober, G. (2015). Upper mesospheric lunar tides over middle and high latitudes during sudden stratospheric warming events. *Journal of Geophysical Research: Space Physics*, *120*, 3084–3096. https://doi.org/10.1002/2015JA020998

Clark, R., Burrage, M., Franke, S., Manson, A., Meek, C., Mitchell, N., & Muller, H. (2002). Observations of 7-d planetary waves with MLT radars and the UARS-HRDI instrument. *Journal of Atmospheric and Solar-Terrestrial Physics*, *64*(8-11), 1217–1228.

Day, K. A., Hibbins, R. E., & Mitchell, N. J. (2011). Aura MLS observations of the westward-propagating s= 1, 16-day planetary wave in the stratosphere, mesosphere and lower thermosphere. *Atmospheric Chemistry and Physics*, *11*(9), 4149–4161.

Day, K. A., & Mitchell, N. (2010). The 16-day wave in the Arctic and Antarctic mesosphere and lower thermosphere. *Atmospheric Chemistry and Physics*, *10*(3), 1461–1472.

Dowdy, A. J., Vincent, R. A., Murphy, D. J., Tsutsumi, M., Riggin, D. M., & Jarvis, M. J. (2004). The large-scale dynamics of the mesosphere–lower thermosphere during the southern hemisphere stratospheric warming of 2002. *Geophysical Research Letters*, *31*, L14102. https://doi.org/10.1029/2004GL020282

Ern, M., Preusse, P., Kalisch, S., Kaufmann, M., & Riese, M. (2013). Role of gravity waves in the forcing of quasi two-day waves in the mesosphere: An observational study. *Journal of Geophysical Research: Atmospheres*, *118*, 3467–3485. https://doi.org/10.1029/2012JD018208

Espy, P., Hibbins, R., Riggin, D., & Fritts, D. (2005). Mesospheric planetary waves over Antarctica during 2002. *Geophysical Research Letters*, *32*, L21804. https://doi.org/10.1029/2005GL023886

Espy, P., Stegman, J., & Witt, G. (1997). Interannual variations of the quasi-16-day oscillation in the polar summer mesospheric temperature. *Journal of Geophysical Research*, *102*(D2), 1983–1990.

Forbes, J. M. (1995). Tidal and planetary waves. *The upper mesosphere and lower thermosphere: A review of experiment and theory*, *87*, 67–87.

Forbes, J. M., Hagan, M., Miyahara, S., Vial, F., Manson, A., Meek, C., & Portnyagin, Y. I. (1995). Quasi 16-day oscillation in the mesosphere and lower thermosphere. *Journal of Geophysical Research*, *100*(D5), 9149–9163.

Forbes, J. M., & Zhang, X. (2015). Quasi-10-day wave in the atmosphere. *Journal of Geophysical Research: Atmospheres*, *120*, 11,079–11,089. https://doi.org/10.1002/2015JD023327

Forbes, J. M., & Zhang, X. (2017). The quasi-6 day wave and its interactions with solar tides. *Journal of Geophysical Research: Space Physics*, *122*, 4764–4776. https://doi.org/10.1002/2017JA023954

Forbes, J. M., Zhang, X., Maute, A., & Hagan, M. E. (2018). Zonally symmetric oscillations of the thermosphere at planetary wave periods. *Journal of Geophysical Research: Space Physics*, *123*, 4110–4128. https://doi.org/10.1002/2018JA025258

Gan, Q., Wang, W., Yue, J., Liu, H., Chang, L. C., Zhang, S., et al. (2016). Numerical simulation of the 6 day wave effects on the ionosphere: Dynamo modulation. *Journal of Geophysical Research: Space Physics*, *121*, 10,103–10,116. https://doi.org/10.1002/2016JA022907

Garcia, R. R., Lieberman, R., Russell, J. M. III, & Mlynczak, M. G. (2005). Large-scale waves in the mesosphere and lower thermosphere observed by SABER. *Journal of the Atmospheric Sciences*, *62*(12), 4384–4399.

Gelaro, R., McCarty, W., Suárez, M. J., Todling, R., Molod, A., Takacs, L., et al. (2017). The Modern-Era Retrospective Analysis for Research and Applications, version 2 (MERRA-2). *Journal of Climate*, *30*(14), 5419–5454.

Gong, Y., Li, C., Ma, Z., Zhang, S., Zhou, Q., Huang, C., et al. (2018). Study of the quasi-5-day wave in the MLT region by a meteor radar chain. *Journal of Geophysical Research: Atmospheres*, *123*, 9474–9487. https://doi.org/10.1029/2018JD029355

Gu, S.-Y., Dou, X., Pancheva, D., Yi, W., & Chen, T. (2018). Investigation of the abnormal quasi 2-day wave activities during the sudden stratospheric warming period of January 2006. *Journal of Geophysical Research: Space Physics*, *123*, 6031–6041. https://doi.org/10.1029/2018JA025596

Gu, S.-Y., Dou, X.-K., Yang, C.-Y., Jia, M., Huang, K.-M., Huang, C.-M., & Zhang, S.-D. (2018). Climatology and anomaly of the quasi-two-day wave behaviors during 2003–2018 austral summer periods. *Journal of Geophysical Research: Space Physics*, *124*, 544–556. https://doi.org/10.1029/2018JA026047

Gu, S.-Y., Li, T., Dou, X., Wang, N.-N., Riggin, D., & Fritts, D. (2013). Long-term observations of the quasi two-day wave by Hawaii MF radar. *Journal of Geophysical Research: Space Physics*, *118*, 7886–7894. https://doi.org/10.1002/2013JA018858

Gu, S.-Y., Li, T., Dou, X., Wu, Q., Mlynczak, M., & Russell III, J. (2013). Observations of quasi-two-day wave by TIMED/SABER and TIMED/TIDI. *Journal of Geophysical Research: Atmospheres*, *118*, 1624–1639. https://doi.org/10.1002/jgrd.50191

Gu, S.-Y., Liu, H.-L., Dou, X., & Li, T. (2016). Influence of the sudden stratospheric warming on quasi-2-day waves. *Atmospheric Chemistry and Physics*, *16*(8), 4885–4896.

Hagan, M., Forbes, J., & Vial, F. (1993). Numerical investigation of the propagation of the quasi-two-day wave into the lower thermosphere. *Journal of Geophysical Research*, *98*(D12), 23,193–23,205.

Harris, T. J., & Vincent, R. A. (1993). The quasi-two-day wave observed in the equatorial middle atmosphere. *Journal of Geophysical Research*, *98*(D6), 10,481–10,490.

Hirooka, T. (2000). Normal mode Rossby waves as revealed by UARS/ISAMS observations. *Journal of the Atmospheric Sciences*, *57*(9), 1277–1285.

Hirooka, T., & Hirota, I. (1985). Normal mode Rossby waves observed in the upper stratosphere. Part II: Second antisymmetric and symmetric modes of zonal wavenumbers 1 and 2. *Journal of the Atmospheric Sciences*, *42*(6), 536–548.

Hirota, I., & Hirooka, T. (1984). Normal mode Rossby waves observed in the upper stratosphere. Part I: First symmetric modes of zonal wavenumbers 1 and 2. *Journal of the Atmospheric Sciences*, *41*(8), 1253–1267.

Hu, J., Ren, R., & Xu, H. (2014). Occurrence of winter stratospheric sudden warming events and the seasonal timing of spring stratospheric final warming. *Journal of the Atmospheric Sciences*, *71*(7), 2319–2334.

Huang, Y., Zhang, S., Li, C., Li, H., Huang, K., & Huang, C. (2017). Annual and interannual variations in global 6.5 DWS from 20 to 110 km during 2002–2016 observed by TIMED/SABER. *Journal of Geophysical Research: Space Physics*, *122*, 8985–9002. https://doi.org/10.1002/2017JA023886

Huang, Y., Zhang, S., Yi, F., Huang, C., Huang, K., Gan, Q., & Gong, Y. (2013). Global climatological variability of quasi-two-day waves revealed by TIMED/SABER observations. *Annales Geophysicae*, *31*, 1061–1075.

Jacobi, C., Schminder, R., & Kürschner, D (1998). Planetary wave activity obtained from long-period (2–18 days) variations of mesopause region winds over central Europe (52°N, 15°E). *Journal of Atmospheric and Solar-Terrestrial Physics*, *60*(1), 81–93.

Jiang, G.-y., Xiong, J.-G., Wan, W.-X., Ning, B.-Q., Liu, L.-B., Vincent, R., & Reid, I. (2005). The 16-day waves in the mesosphere and lower thermosphere over Wuhan (30.6°N, 114.5°E) and Adelaide (35°S, 138°E). *Advances in Space Research*, *35*(11), 2005–2010.

Jiang, G.-y., Xu, J., Xiong, J., Ma, R., Ning, B., Murayama, Y., et al. (2008). A case study of the mesospheric 6.5-day wave observed by radar systems. *Journal of Geophysical Research*, *113*, D16111. https://doi.org/10.1029/2008JD009907

John, S. R., & Kumar, K. K. (2016). Global normal mode planetary wave activity: A study using TIMED/SABER observations from the stratosphere to the mesosphere-lower thermosphere. *Climate Dynamics*, *47*(12), 3863–3881.

Kasahara, A. (1976). Normal modes of ultralong waves in the atmosphere. *Monthly Weather Review*, *104*(6), 669–690.

Kasahara, A. (1980). Effect of zonal flows on the free oscillations of a barotropic atmosphere. *Journal of the Atmospheric Sciences*, *37*(5), 917–929.

Kingsley, S., Muller, H., Nelson, L., & Scholefield, A. (1978). Meteor winds over Sheffield (53°N, 2°W). *Journal of Atmospheric and Terrestrial Physics*, *40*(8), 917–922.

Kishore, P., Namboothiri, S., Igarashi, K., Gurubaran, S., Sridharan, S., Rajaram, R., & Ratnam, M. V. (2004). MF radar observations of 6.5-day wave in the equatorial mesosphere and lower thermosphere. *Journal of Atmospheric and Solar-Terrestrial Physics*, *66*(6-9), 507–515.

Koval, A., Gavrilov, N., Pogoreltsev, A., & Shevchuk, N. (2018). Propagation of stationary planetary waves to the thermosphere at different levels of solar activity. *Journal of Atmospheric and Solar-Terrestrial Physics*, *173*, 140–149.

Kovalam, S., Vincent, R. A., Reid, I. M., Tsuda, T., Nakamura, T., Ohnishi, K., et al. (1999). Longitudinal variations in planetary wave activity in the equatorial mesosphere. *Earth, Planets and Space*, *51*(7-8), 665–674.

Krüger, K., Naujokat, B., & Labitzke, K. (2005). The unusual midwinter warming in the Southern Hemisphere stratosphere 2002: A comparison to Northern Hemisphere phenomena. *Journal of the Atmospheric Sciences*, *62*(3), 603–613.

Labitzke, K., & Van Loon, H. (1999). *The stratosphere: Phenomena, history, and relevance*. New York: Springer Science & Business Media.

Lieberman, R., Riggin, D., Franke, S., Manson, A., Meek, C., Nakamura, T., et al. (2003). The 6.5-day wave in the mesosphere and lower thermosphere: Evidence for baroclinic/barotropic instability. *Journal of Geophysical Research*, *108*(D20), 4640. https://doi.org/10.1029/2002JD003349

Limpasuvan, V., & Wu, D. L. (2003). Two-day wave observations of UARS Microwave Limb Sounder mesospheric water vapor and temperature. *Journal of Geophysical Research*, *108*(D10), 4307. https://doi.org/10.1029/2002JD002903

Limpasuvan, V., & Wu, D. L. (2009). Anomalous two-day wave behavior during the 2006 austral summer. *Geophysical Research Letters*, *36*, L04807. https://doi.org/10.1029/2008GL036387

Limpasuvan, V., Wu, D. L., Schwartz, M. J., Waters, J. W., Wu, Q., & Killeen, T. L. (2005). The two-day wave in EOS MLS temperature and wind measurements during 2004–2005 winter. *Geophysical Research Letters*, *32*, L17809. https://doi.org/10.1029/2005GL023396

Liu, H.-L., Talaat, E., Roble, R., Lieberman, R., Riggin, D., & Yee, J.-H. (2004). The 6.5-day wave and its seasonal variability in the middle and upper atmosphere. *Journal of Geophysical Research*, *109*, D21112. https://doi.org/10.1029/2004JD004795

Livesey, N., Read, W. G., Wagner, P. A., Froidevaux, L., Lambert, A., Manney, G. L., et al. (2017). Aura Microwave Limb Sounder(MLS) version4.2x level 2 data quality and description document, JPL D-33509Rev. C.

Luo, Y., Manson, A., Meek, C., Meyer, C., Burrage, M., Fritts, D., et al. (2002). The 16-day planetary waves: Multi-MF radar observations from the arctic to equator and comparisons with the HRDI measurements and the GSWM modelling results. *Annales Geophysicae*, *20*, 691–709.

Luo, Y., Manson, A. H., Meek, C. E., Meyer, C. K., & Forbes, J. M. (2000). The quasi 16-day oscillations in the mesosphere and lower thermosphere at Saskatoon (52°N, 107°W), 1980–1996. *Journal of Geophysical Research*, *105*(D2), 2125–2138.

Luo, Y., Manson, A., Meek, C., Thayaparan, T., MacDougall, J., & Hocking, W. (2002). The 16-day wave in the mesosphere and lower thermosphere: Simultaneous observations at Saskatoon (52°N, 107°W) and London (43°N, 81°W), canada. *Journal of Atmospheric and Solar-Terrestrial Physics*, *64*(8-11), 1287–1307.

Ma, Z., Gong, Y., Zhang, S., Zhou, Q., Huang, C., Huang, K., et al. (2017). Responses of quasi 2 day waves in the MLT region to the 2013 SSW revealed by a meteor radar chain. *Geophysical Research Letters*, *44*, 9142–9150. https://doi.org/10.1002/2017GL074597

Madden, R. A. (1979). Observations of large-scale traveling Rossby waves. *Reviews of Geophysics*, *17*(8), 1935–1949.

Madden, R. A. (2007). Large-scale, free Rossby waves in the atmosphere-an update. *Tellus A: Dynamic Meteorology and Oceanography*, *59*(5), 571–590.

Manney, G. L., Krüger, K., Pawson, S., Minschwaner, K., Schwartz, M. J., Daffer, W. H., et al. (2008). The evolution of the stratopause during the 2006 major warming: Satellite data and assimilated meteorological analyses. *Journal of Geophysical Research*, *113*, D11115. https://doi.org/10.1029/2007JD009097

Manney, G. L., Schwartz, M. J., Krüger, K., Santee, M. L., Pawson, S., Lee, J. N., et al. (2009). Aura Microwave Limb Sounder observations of dynamics and transport during the record-breaking 2009 Arctic stratospheric major warming. *Geophysical Research Letters*, *36*, L12815. https://doi.org/10.1029/2009GL038586

Matthias, V., Dörnbrack, A, & Stober, G. (2016). The extraordinarily strong and cold polar vortex in the early northern winter 2015/2016. *Geophysical Research Letters*, *43*, 12,287–12,294. https://doi.org/10.1002/2016GL071676

Matthias, V., & Ern, M. (2018). On the origin of the mesospheric quasi-stationary planetary waves in the unusual arctic winter 2015/2016. *Atmospheric Chemistry and Physics*, *18*(7), 4803–4815.

Matthias, V., Hoffmann, P., Rapp, M., & Baumgarten, G. (2012). Composite analysis of the temporal development of waves in the polar MLT region during stratospheric warmings. *Journal of Atmospheric and Solar-Terrestrial Physics*, *90*, 86–96.

McCormack, J. P., Coy, L., & Hoppel, K. W. (2009). Evolution of the quasi 2-day wave during January 2006. *Journal of Geophysical Research*, *114*, D20115. https://doi.org/10.1029/2009JD012239

McDonald, A., Hibbins, R. E., & Jarvis, M. J. (2011). Properties of the quasi 16 day wave derived from EOS MLS observations. *Journal of Geophysical Research*, *116*, D06112. https://doi.org/10.1029/2010JD014719

Meek, C., & Manson, A. (2009). Summer planetary-scale oscillations: Aura MLS temperature compared with ground-based radar wind (pp. 1763–1774).

Merzlyakov, E., Solovjova, T., & Yudakov, A. (2013). The interannual variability of a 5–7 day wave in the middle atmosphere in autumn from era product data, aura MLS data, and meteor wind data. *Journal of Atmospheric and Solar-Terrestrial Physics*, *102*, 281–289.

Meyer, C. K., & Forbes, J. M. (1997). A 6.5-day westward propagating planetary wave: Origin and characteristics. *Journal of Geophysical Research*, *102*(D22), 26,173–26,178.

Mitchell, N., Middleton, H., Beard, A., Williams, P., & Muller, H. (1999). The 16-day planetary wave in the mesosphere and lower thermosphere. *Annales Geophysicae*, *17*, 1447–1456.

Miyoshi, Y. (1999). Numerical simulation of the 5-day and 16-day waves in the mesopause region. *Earth, Planets and Space*, *51*(7-8), 763–772.

Miyoshi, Y., & Hirooka, T. (1999). A numerical experiment of excitation of the 5-day wave by a GCM. *Journal of the atmospheric sciences*, *56*(11), 1698–1707.

Moudden, Y., & Forbes, J. (2014). Quasi-two-day wave structure, interannual variability, and tidal interactions during the 2002–2011 decade. *Journal of Geophysical Research: Atmospheres*, *119*, 2241–2260. https://doi.org/10.1002/2013JD020563

Muller, H., & Nelson, L. (1978). A travelling quasi 2-day wave in the meteor region. *Journal of Atmospheric and Terrestrial Physics*, *40*(6), 761–766.

Nozawa, S., Imaida, S., Brekke, A., Hall, C., Manson, A., Meek, C., et al. (2003). The quasi 2-day wave observed in the polar mesosphere. *Journal of Geophysical Research*, *108*(D2), 4039. https://doi.org/10.1029/2002JD002440

Offermann, D., Hoffmann, P., Knieling, P., Koppmann, R., Oberheide, J., Riggin, D., et al. (2011). Quasi 2 day waves in the summer mesosphere: Triple structure of amplitudes and long-term development. *Journal of Geophysical Research*, *116*, D00P02. https://doi.org/10.1029/2010JD015051

Palo, S., Roble, R., & Hagan, M. (1998). TIME-GCM results for the quasi-two-day wave. *Geophysical Research Letters*, *25*(20), 3783–3786.

Palo, S. E., Roble, R. G., & Hagan, M. E. (1999). Middle atmosphere effects of the quasi-two-day wave determined from a general circulation model. *Earth, Planets and Space*, *51*(7-8), 629–647.

Pancheva, D., & Mukhtarov, P. (2011). Atmospheric tides and planetary waves: Recent progress based on SABER/TIMED temperature measurements (2002–2007). In *Aeronomy of the Earth's atmosphere and ionosphere* (pp. 19–56). New York: Springer.

Pancheva, D., Mukhtarov, P., Andonov, B., & Forbes, J. (2010). Global distribution and climatological features of the 5–6-day planetary waves seen in the SABER/TIMED temperatures (2002–2007). *Journal of Atmospheric and Solar-Terrestrial Physics*, *72*(1), 26–37.

Pancheva, D., Mukhtarov, P., Mitchell, N., Fritts, D., Riggin, D., Takahashi, H., et al. (2008). Planetary wave coupling (5–6-day waves) in the low-latitude atmosphere–ionosphere system. *Journal of Atmospheric and Solar-Terrestrial Physics*, *70*(1), 101–122.

Pancheva, D., Mukhtarov, P., Mitchell, N., Merzlyakov, E., Smith, A., Andonov, B., et al. (2008). Planetary waves in coupling the stratosphere and mesosphere during the major stratospheric warming in 2003/2004. *Journal of Geophysical Research*, *113*, D12105. https://doi.org/10.1029/2007JD009011

Pancheva, D., Mukhtarov, P., & Siskind, D. E. (2018a). Climatology of the quasi-2-day waves observed in the MLS/Aura measurements (2005–2014). *Journal of Atmospheric and Solar-Terrestrial Physics*, *171*, 210–224.

Pancheva, D., Mukhtarov, P., & Siskind, D. E. (2018b). The quasi-6-day waves in NOGAPS-ALPHA forecast model and their climatology in MLS/Aura measurements (2005–2014). *Journal of Atmospheric and Solar-Terrestrial Physics*, *181*, 19–37.

Pedatella, N., Liu, H.-L., & Hagan, M. (2012). Day-to-day migrating and nonmigrating tidal variability due to the six-day planetary wave. *Journal of Geophysical Research*, *117*, A06301. https://doi.org/10.1029/2012JA017581

Riggin, D. M., Liu, H.-L., Lieberman, R. S., Roble, R. G., Russell Iii, J. M., Mertens, C. J., et al. (2006). Observations of the 5-day wave in the mesosphere and lower thermosphere. *Journal of Atmospheric and Solar-Terrestrial Physics*, *68*(3-5), 323–339.

Rodgers, C. (1976). Evidence for the five-day wave in the upper stratosphere. *Journal of the Atmospheric Sciences*, *33*(4), 710–711.

Rodgers, C., & Prata, A. (1981). Evidence for a traveling two-day wave in the middle atmosphere. *Journal of Geophysical Research*, *86*(C10), 9661–9664.

Salby, M. L. (1980). The influence of realistic dissipation on planetary normal structures. *Journal of the Atmospheric Sciences*, *37*(10), 2186–2199.

Salby, M. L. (1981a). Rossby normal modes in nonuniform background configurations. Part I: Simple fields. *Journal of the Atmospheric Sciences*, *38*(9), 1803–1826.

Salby, M. L. (1981b). Rossby normal modes in nonuniform background configurations. Part II. Equinox and solstice conditions. *Journal of the Atmospheric Sciences*, *38*(9), 1827–1840.

Salby, M. L. (1984). Survey of planetary-scale traveling waves: The state of theory and observations. *Reviews of Geophysics*, *22*(2), 209–236.

Salby, M. L., & Callaghan, P. F. (2001). Seasonal amplification of the 2-day wave: Relationship between normal mode and instability. *Journal of the Atmospheric Sciences*, *58*(14), 1858–1869.

Salby, M. L., & Roper, R. (1980). Long-period oscillations in the meteor region. *Journal of the Atmospheric Sciences*, *37*(1), 237–244.

Sandford, D., Schwartz, M., & Mitchell, N. J. (2008). The wintertime two-day wave in the polar stratosphere, mesosphere and lower thermosphere. *Atmospheric Chemistry and Physics*, *8*(3), 749–755.

Sassi, F., Garcia, R., & Hoppel, K. (2012). Large-scale Rossby normal modes during some recent Northern Hemisphere winters. *Journal of the Atmospheric Sciences*, *69*(3), 820–839.

Sato, K., & Nomoto, M. (2015). Gravity wave–induced anomalous potential vorticity gradient generating planetary waves in the winter mesosphere. *Journal of the Atmospheric Sciences*, *72*(9), 3609–3624.

Schwartz, M., Lambert, A., Manney, G., Read, W., Livesey, N., Froidevaux, L., et al. (2008). Validation of the aura Microwave Limb Sounder temperature and geopotential height measurements. *Journal of Geophysical Research*, *113*, D15S11. https://doi.org/10.1029/2007JD008783

Siddiqui, T. A., Stolle, C., Lühr, H., & Matzka, J. (2015). On the relationship between weakening of the northern polar vortex and the lunar tidal amplification in the equatorial electrojet. *Journal of Geophysical Research: Space Physics*, *120*, 10,006–10,019. https://doi.org/10.1002/2015JA021683

Sridharan, S., Sathishkumar, S., & Gurubaran, S. (2009). Variabilities of mesospheric tides and equatorial electrojet strength during major stratospheric warming events. *Annales Geophysicae*, *27*, 4125–4130.

Stober, G., Matthias, V., Jacobi, C., Wilhelm, S., Höffner, J., Chau, J. L., & Annales geophysicae (2017). Exceptionally strong summer-like zonal wind reversal in the upper mesosphere during winter 2015/16, *35*, 711–720.

Talaat, E., Yee, J.-H., & Zhu, X. (2001). Observations of the 6.5-day wave in the mesosphere and lower thermosphere. *Journal of Geophysical Research*, *106*(D18), 20,715–20,723.

Tsuda, T., Kato, S., & Vincent, RAo (1988). Long period wind oscillations observed by the kyoto meteor radar and comparison of the quasi-2-day wave with adelaide HF radar observations. *Journal of Atmospheric and Terrestrial Physics*, *50*(3), 225–230.

Tunbridge, V. M., Sandford, D. J., & Mitchell, N. J. (2011). Zonal wave numbers of the summertime 2 day planetary wave observed in the mesosphere by EOS aura Microwave Limb Sounder. *Journal of Geophysical Research*, *116*, D11103. https://doi.org/10.1029/2010JD014567

Wang, H., Boyd, J. P., & Akmaev, R. A. (2016). On computation of hough functions. *Geoscientific Model Development*, *9*(4), 1477–1488.

Waters, J. W., Froidevaux, L., Harwood, R. S., Jarnot, R. F., Pickett, H. M., Read, W. G., et al. (2006). The earth observing system Microwave Limb Sounder (EOS MLS) on the aura satellite. *IEEE Transactions on Geoscience and Remote Sensing*, *44*(5), 1075–1092.

Williams, C., & Avery, S. (1992). Analysis of long-period waves using the mesosphere-stratosphere-troposphere radar at poker flat, alaska. *Journal of Geophysical Research*, *97*(D18), 20,855–20,861.

Wu, D., Fishbein, E., Read, W., & Waters, J. (1996). Excitation and evolution of the quasi-2-day wave observed in UARS/MLS temperature measurements. *Journal of the Atmospheric Sciences*, *53*(5), 728–738.

Wu, D., Hays, P., & Skinner, W. (1994). Observations of the 5-day wave in the mesosphere and lower thermosphere. *Geophysical Research Letters*, *21*(24), 2733–2736.

Wu, D., Hays, P., Skinner, W., Marshall, A., Burrage, M., Lieberman, R., & Ortland, D. (1993). Observations of the quasi 2-day wave from the high resolution doppler imager on UARS. *Geophysical Research Letters*, *20*(24), 2853–2856.

Xiong, J., Wan, W., Ding, F., Liu, L., Hu, L., & Yan, C. (2018). Two day wave traveling westward with wave number 1 during the sudden stratospheric warming in January 2017. *Journal of Geophysical Research: Space Physics*, *123*, 3005–3013. https://doi.org/10.1002/2017JA025171

Yamazaki, Y. (2018). Quasi-6-day wave effects on the equatorial ionization anomaly over a solar cycle. *Journal of Geophysical Research: Space Physics*, *123*, 9881–9892. https://doi.org/10.1029/2018JA026014

Yamazaki, Y., Kosch, M. J., & Emmert, J. T. (2015). Evidence for stratospheric sudden warming effects on the upper thermosphere derived from satellite orbital decay data during 1967–2013. *Geophysical Research Letters*, *42*, 6180–6188. https://doi.org/10.1002/2015GL065395

Yue, J., Liu, H.-L., & Chang, L. C. (2012). Numerical investigation of the quasi 2 day wave in the mesosphere and lower thermosphere. *Journal of Geophysical Research*, *117*, D05111. https://doi.org/10.1029/2011JD016574

Zhang, X., & Forbes, J. M. (2014). Lunar tide in the thermosphere and weakening of the northern polar vortex. *Geophysical Research Letters*, *41*, 8201–8207. https://doi.org/10.1002/2014GL062103